

## Core polarization and the structure of simple metals

K. K. Mon, N. W. Ashcroft, and G. V. Chester

*Laboratory of Atomic and Solid State Physics and Materials Science Center, Cornell University, Ithaca, New York 14853*

(Received 20 November 1978)

Many liquid simple metals (Ga and Sn are prominent examples) have static structure factors  $S(k)$  that appear to depart appreciably from the predictions of standard central-force models of liquid structure. The inferred structural anomalies take the form of weak subsidiary maxima on  $S(k)$  near the principal diffraction peak, or even asymmetries in the peak itself. They are shown here to be a consequence of corresponding structure introduced into the effective ion-ion interaction by the inclusion of dynamically screened fluctuating dipole interactions between ion cores. The effects are therefore most pronounced in ions that are highly polarizable and in extreme cases actually manifest themselves as nonmonotonic contributions to the pair potential at relatively short range. Less extreme behavior can result merely in a softening of the standard pseudopotential-based pair interaction calculated in the absence of such terms. A calculation of the effective ion-ion potential therefore requires a knowledge of the frequency-dependent ionic and electron gas polarizabilities and the one-electron pseudopotential. Model potentials based on reasonable estimates of all of these are used in conjunction with simulation (Monte Carlo) methods to show that the structural anomalies can indeed be attributed to core-polarization effects.

### I. INTRODUCTION

X-ray and neutron-scattering techniques have now developed to the point where extremely accurate static structure factors are available for a wide range of liquid metals and many of their alloys.<sup>1</sup> Theoretical progress in understanding the structure of liquid metals as revealed by such measurements has been greatly aided by the parallel development of numerical methods which permit, at least within the model of pair interactions, the calculation of both equilibrium and non equilibrium properties.<sup>2</sup> For many structural purposes, it is well known that pair potentials can be defined in the metallic state. In simple metals (that is, nontransition metals) to which we restrict attention, the interactions corresponding to these potentials are regarded as the sum of direct Coulomb forces between rigid *point* ions, and an indirect term originating with the conduction electrons which incorporates the pseudopotential. This is a response contribution and as far as the conduction electrons are concerned reflects the finite size and structure of the ion.

The assumption that the *direct* interaction never departs seriously from Coulomb's law is normally justified on the grounds that the mean equilibrium separation between the ions is largely determined by energy considerations applied to the *conduction electrons*. Such separations are, for the simple metals, much in excess of the ionic diameters.<sup>3</sup> This view takes the ion to be an inert object: it ignores the possibility of fluctuation or polarization effects, the most pronounced of which are the dispersion or Van der Waals forces. The fact that these effects, so important in the understand-

ing of the condensed noble gases, can be neglected in metals is attributed to the assumption that in simple metals, at any rate, the ion cores are considered to be not very polarizable. Given the overwhelming strength of the Coulomb interaction itself, Van der Waals-type interactions are thought to be of only minor importance.

The purpose of this paper is to show that for a certain class of simple metals the appropriately screened interactions arising from core-polarization effects<sup>4</sup> are not at all unimportant when compared with pseudopotential-based pair interactions.<sup>5</sup> The latter incorporate the fairly complete effects of screening, and it is to the somewhat weak net result that comparison of core-polarization effects should properly be made, rather than to the strong unscreened Coulomb interaction itself. The importance of screened Van der Waals interactions as contributors to the thermodynamic functions<sup>5</sup> of metals has already been stressed. Here we shall concentrate on their possible *structural* consequences, and we shall dwell particularly on their manifestations in the liquid state. This requires us to examine the static structure factor  $S(k)$  which, as in the case for most simple classical liquids can be broadly accounted for by the hard-sphere model representing simple geometrical exclusion.<sup>6</sup> There are, however, noticeable deviations from the predictions of this model,<sup>7</sup> particularly in certain polyvalent metals, (Ga,<sup>8</sup> Ge,<sup>9</sup> Sb,<sup>10</sup> Bi,<sup>11</sup> Sn,<sup>12</sup> Hg,<sup>13</sup> Zn,<sup>14</sup> and <sup>15</sup>Cd).<sup>16</sup> These deviations may take the extreme form of subsidiary maxima in the vicinity of the principal diffraction peak, or less prominently as asymmetries of varying degrees in the peak itself. (Smaller distortions of second and

higher diffraction peaks have also been reported.<sup>12)</sup> Somewhat less apparent still is an inferred anomaly associated with certain of the alkali metals (rubidium and sodium, for example). Here it has been noted<sup>17,18</sup> that in a comparison of their structure factors with (i) simulation studies of systems interacting via  $r^{-4}$ -type potentials and (ii) experimental measurements of  $S(k)$  for liquid argon, there appears to be the possibility that the ion-ion short-range interaction is really quite soft. But inspection of this region in the calculated ion-ion interactions<sup>19</sup> from pseudopotential theory shows the opposite: in the relevant energy range the ion-ion interaction appears just as steep as, for example, a Lennard-Jones potential.

These are examples of departures from "expected behavior" and as a possible cause for the discrepancies we shall propose the core-polarization effects normally neglected in the treatments of pair interactions in simple metals. As we shall argue below, fluctuating dipole contributions to pair interactions, even after screening by the valence-electron gas, appear to be significant, especially at short range, and in precisely those simple metals displaying anomalous behavior in their liquid structures. To support this proposition we will consider, in Sec. II, an extension of recent calculations of *screened* Van der Waals interactions.<sup>5</sup> The treatment incorporates pseudopotential effects and therefore more properly allows the electron gas to be treated as a quasi-uniform responding medium. In discussing the response of this medium to core fluctuations we will need its frequency-dependent polarizability and to include, at least approximately, dynamic exchange. This is not a straightforward matter and is dealt with only approximately in Sec. III. Effective ion-ion interactions that account for inner-core (Pauli) repulsion, screened pseudopotential, and screened core-polarization effects are also presented in Sec. III. Monte Carlo calculations with these potentials are described in Sec. IV and these provide the most direct evidence to show that the structural anomalies are attributable to the core-polarization terms. In the case of those polyvalent metals with highly polarizable cores, we find it possible for these terms to introduce prominent nonmonotonic features into otherwise short-range-repulsive long-range-attractive potentials. Gallium is a very strong case in point and one on which we largely concentrate.

## II. ION-ION INTERACTIONS AND SCREENED CORE-POLARIZATION EFFECTS

We begin this section by first establishing the many-body Hamiltonian for the system that will

form the basis of the perturbation calculation of the effective ion-ion interactions. The electrons in the system are considered divided into two classes: localized core electrons ( $Z_i$  on each ion), and valence electrons ( $Z = Z_A - Z_i$ , per atom, where  $Z_A$  is the atomic number). Note immediately that this implied site distinguishability of electrons is tantamount to a description of the system in terms of a Hartree-type product state of many-electron core functions. It is not properly symmetrized with respect to exchange of identical electrons between *different* ions. The state is used however, on the understanding that the neglected core-core exchange effects can ultimately be incorporated as a highly repulsive contribution to the short-range ion-ion potential (the inner short-range "Pauli repulsion"). There must also be a core-valence exchange contribution: we will return to this when we discuss the character of the valence-electron states.

Let  $\vec{R}$  denote the position of a nucleus of an ion. We introduce a density operator for the ion at  $\vec{R}$

$$\hat{\rho}_{\vec{R}}^{\pm}(\vec{r}) = Z_A \delta(\vec{r} - \vec{R}) - \sum_{i=1}^{Z_i} \delta(\vec{r} - \vec{R} - \vec{r}_{\vec{R},i}^{\pm}), \quad (1)$$

where the  $\vec{r}_{\vec{R},i}^{\pm}$  denote the coordinates of those bound electrons assigned to the ion at  $\vec{R}$ . Note that  $|e|$  times (1) gives the total charge-density operator (nuclear plus electronic). Further, suppose  $\Phi_{\vec{R}}^0$  is the localized  $Z_i$ -electron ground state of the electrons on the ion at  $\vec{R}$ . Then  $\langle \Phi_{\vec{R}}^0 | \hat{\rho}_{\vec{R}}^{\pm} | \Phi_{\vec{R}}^0 \rangle$  approaches the valence  $Z$  at distances from the ion much larger than the ion size. It follows that

$$\begin{aligned} \hat{\rho}_{\vec{R}}^{\pm}(\vec{q}) &= e^{i\vec{q} \cdot \vec{R}} \left( Z + \sum_{i=1}^{Z_i} (1 - e^{i\vec{q} \cdot \vec{r}_{\vec{R},i}^{\pm}}) \right) \\ &= Z e^{i\vec{q} \cdot \vec{R}} + \hat{\nu}_{\vec{R}}^{\pm}(\vec{q}) \end{aligned} \quad (2)$$

can be regarded as an operator describing density fluctuations (about a valence  $Z$ ) for an ion located at  $\vec{R}$ .

Given (1) it is a straightforward matter to write the Hamiltonian for the system. We consider  $N$  identical ions in a volume  $\Omega$ . There is an ionic Hamiltonian  $H_{\vec{R}}$  assigned to each site  $\vec{R}$  and

$$H_{\vec{R}} \Phi_{\vec{R}}^n = \epsilon_{\text{ion}}^n \Phi_{\vec{R}}^n, \quad (3)$$

$\Phi_{\vec{R}}^0$  being the ground state as described above. If the valence-electron coordinates are  $\vec{r}_j$ , then their corresponding density operator is

$$\hat{\rho}^v(\vec{q}) = - \sum_{j=1}^{NZ} e^{i\vec{q} \cdot \vec{r}_j} \quad (4)$$

(again,  $|e|$  times this gives the charge density). We take  $H_0$  to be the noninteracting Hamiltonian for this system. ( $H_0 = \sum_{j=1}^{NZ} p_j^2 / 2m$ .)

Let  $v_c(q) = 4\pi e^2 / q^2$  be the Fourier transform of

the Coulomb interaction. The Hamiltonian for the entire interacting system in the approximation described above is then

$$H = H_v + \sum_{\vec{R}} H_{\vec{R}} + \frac{1}{2\Omega} \sum_{\vec{R}, \vec{R}', q} \hat{\rho}_{\vec{R}}^{\dagger}(\vec{q}) \hat{\rho}_{\vec{R}'}^{\dagger}(-\vec{q}) v_c(q) + \frac{1}{\Omega} \sum_{\vec{R}, \vec{q}} \hat{\rho}_{\vec{R}}^{\dagger}(\vec{q}) \hat{\rho}^v(-\vec{q}) v_c(q) + \frac{1}{2\Omega} \sum_{\vec{q}} \hat{\rho}^v(\vec{q}) \hat{\rho}^v(-\vec{q}) v_c(q) \quad (5)$$

or

$$H = H_0 + H_1,$$

where

$$H_0 = H_v + \sum_{\vec{R}} H_{\vec{R}} \quad (6)$$

describes the unperturbed systems and,

$$H_1 = \sum_{\vec{q}} \frac{v_c(q)}{\Omega} \left( \sum_{\vec{R}, \vec{R}'} \frac{1}{2} \hat{\rho}_{\vec{R}}^{\dagger}(\vec{q}) \hat{\rho}_{\vec{R}'}^{\dagger}(-\vec{q}) + \sum_{\vec{R}} \hat{\rho}_{\vec{R}}^{\dagger}(\vec{q}) \hat{\rho}^v(-\vec{q}) + \frac{1}{2} \hat{\rho}^v(\vec{q}) \hat{\rho}^v(-\vec{q}) \right) \quad (7)$$

couple the systems together. We note, for example, that in the absence of the valence electrons, the first term in (7), in the approximation of localized core states, will give rise in lowest order to the familiar London interactions.<sup>5</sup>

The Hamiltonian (5) can be related to the one normally written in the pseudopotential approach to ion-ion interactions in metals as follows: Let

$$\Psi = \Psi^v \prod_{\vec{R}} \Phi_{\vec{R}}^0 \quad (8)$$

represent a normalized Hartree-type state describing the electron gas and the  $N$ -ions in their ground states. Then the expectation value of  $H$  in such a state is

$$\sum_{\vec{R}} \mathcal{E}_{\text{ion}}^0 + \frac{1}{2\Omega} \sum_{\vec{q}} v_c(q) \bar{\rho}^{\dagger}(-\vec{q}) \bar{\rho}^{\dagger}(-\vec{q}) + \langle \Psi^v | \left( H_v - \frac{1}{\Omega} \sum_{\vec{q}} v_c(q) \bar{\rho}^{\dagger}(\vec{q}) \hat{\rho}^v(-\vec{q}) + \frac{1}{2\Omega} \sum_{\vec{q}} v_c(q) \hat{\rho}^v(\vec{q}) \hat{\rho}^v(-\vec{q}) \right) | \Psi^v \rangle, \quad (9)$$

where

$$\bar{\rho}^{\dagger}(\vec{q}) = \sum_{\vec{R}} Z e^{i\vec{q} \cdot \vec{R}} \left( 1 + \frac{1}{Z} \sum_{i=1}^{Z_i} \langle \Phi^0 | (1 - e^{i\vec{q} \cdot \vec{r}_{\vec{R}, i}}) | \Phi^0 \rangle \right) = Z \sum_{\vec{R}} e^{i\vec{q} \cdot \vec{R}} + O(q^2)$$

if the ions are compact and well separated, as we

shall suppose. The second term in (9) is therefore the familiar

$$\frac{1}{2\Omega} \sum_{\vec{R}, \vec{R}'} \frac{4\pi Z^2 e^2}{q^2} e^{i\vec{q} \cdot (\vec{R} - \vec{R}')}$$

arising from point rigid ions of charge  $Ze$ , plus small corrections arising from their finite size. In a similar way the fourth term of (9) could be cast in a form with leading term

$$\frac{1}{\Omega} \sum_{\vec{q}} \sum_{\vec{R}} e^{i\vec{q} \cdot \vec{R}} \left( \frac{-4\pi e^2 Z}{q^2} \right) \hat{\rho}^v(-\vec{q}), \quad (10)$$

that is to say, a coupling of the valence electrons to *point* ions of charge  $Ze$ . However, what normally appears in place of (10), in pseudopotential theory is

$$\frac{1}{\Omega} \sum_{\vec{q}} \sum_{\vec{R}} e^{i\vec{q} \cdot \vec{R}} v_{ps}(q) \hat{\rho}^v(-\vec{q}) \quad (11)$$

which physically reflects the fact that while the intent is to exploit the properties of the valence-electron system as though it were nearly uniform, the requirements of orthogonality of the valence states to the states described by  $\Phi_{\vec{R}}^0$  force it to be very nonuniform near the ions themselves. As is well known,<sup>3</sup> however, it is formally possible to regard the valence-electron system as quasiuniform (particularly in the response sense) providing that in any one-electron treatment the potential between valence electrons and core is replaced by a pseudopotential  $v_{ps}(q)$ , as in (11). We shall make this assumption here (and also that the pseudopotential is local, as written). In any one-electron theory of the system, a local approximation to the core-valence exchange terms mentioned above must also eventually reside in  $v_{ps}$ . Thus if (8) is chosen as the state describing the system, with  $\Psi^v$  interpreted as a many-electron valence-electron state with core-space inhomogeneities removed, then we may regard

$$H - \sum_{\vec{R}} \mathcal{E}_{\text{ion}}^0 = \frac{1}{2\Omega} \sum_{\vec{q} \neq 0} v_c(q) \bar{\rho}^{\dagger}(\vec{q}) \bar{\rho}^{\dagger}(-\vec{q}) + \sum_j \frac{p_{\vec{q}}^2}{2m} + \frac{1}{2\Omega} \sum_{\vec{q} \neq 0} v_c(q) \hat{\rho}^v(\vec{q}) \hat{\rho}^v(-\vec{q}) + \frac{1}{\Omega} \sum_{\vec{q} \neq 0} v_{ps}(q) \bar{\rho}^{\dagger}(\vec{q}) \bar{\rho}^{\dagger}(-\vec{q}) + E_0 \quad (12)$$

as the Hamiltonian for valence electrons. The quantity  $E_0$  in (12) is the aggregate of all  $q=0$  terms in the problem as discussed by Ashcroft and Langreth.<sup>19</sup> When these are separated out the first term on the right-hand side in (12) is the Madelung energy  $E_M$  and the second and third terms are recognized as the standard interacting-elec-

tron-gas Hamiltonian. The right-hand side of (12) is the starting point for the development of the thermodynamic functions of simple metals in which either by diagrammatic perturbation theory<sup>5</sup> (see below) or by considering the electron gas as a nonlinear dielectric, the energy or related thermodynamic quantities can be developed in orders of  $v_{ps}$ . For most practical purposes the electron system can be taken in its ground state in which case the lowest-order result for the energy is

$$E = E_{EG} + E_M + E_0 + \frac{N}{2\Omega} \times \sum_{\vec{q} \neq 0} |v_{ps}(q)|^2 \left( \frac{1}{\epsilon(q, 0)} - 1 \right) \bar{\rho}^i(\vec{q}) \bar{\rho}^i(-\vec{q}) \left( \frac{4\pi Z^2 e^2}{q^2} \right) \times \left( \frac{1}{Z v_c(q)} \right)^2, \quad (13)$$

where  $E_{EG}$  is the ground-state energy of the electron gas and is just a function of volume. In (13),  $\epsilon(q, 0)$  is the static dielectric function of the electron gas. Note that this is a linear-response result in which the electron-ion coupling is included to first order but the electron-electron interaction is included to all orders. From the present viewpoint, the significant aspect of (13) is the fact that apart from a one-body term, the quantity involving  $|v_{ps}|^2$  can be combined with  $E_M$  to give

$$\frac{1}{2} \frac{N}{\Omega} \sum_{\vec{q} \neq 0} \frac{4\pi Z^2 e^2}{q^2} \left[ 1 + \left( \frac{v_{ps}(q)}{Z v_c(q)} \right)^2 \left( \frac{1}{\epsilon(q, 0)} - 1 \right) \right] \times \left( \frac{1}{N} \hat{v}^i(\vec{q}) \hat{v}^i(-\vec{q}) - 1 \right) = \frac{1}{2} \frac{N}{\Omega} \sum_{\vec{q} \neq 0} \Phi_{ps}(q) \left( \frac{1}{N} \hat{v}^i(\vec{q}) \hat{v}^i(-\vec{q}) - 1 \right), \quad (14)$$

where  $\hat{v}^i(\vec{q}) = Z^{-1} \bar{\rho}^i(\vec{q})$  is the nuclear-density operator. The form of (14) shows that

$$\Phi_{ps}(q) = \frac{4\pi Z^2 e^2}{q^2} \left[ 1 + \left( \frac{v_{ps}(q)}{Z v_c(q)} \right)^2 \left( \frac{1}{\epsilon(q, 0)} - 1 \right) \right] \quad (15)$$

$$= \frac{4\pi Z^2 e^2}{q^2} + v_{ps}(q) \Pi(q, 0) v_{ps}(q) \quad (16)$$

is the Fourier transform (except<sup>19</sup> for  $q=0$ ) of a pair interaction between ions consisting of a direct  $Z^2(e^2/r)$  as appropriate to well-separated "point" ions, and a response term [involving the electron-gas static polarizability  $\Pi(q, 0)$ ] arising from the coupling of the ions to the electron gas via the pseudopotential. These various terms are shown graphically in Figs. 1(a) and 1(b). The sum of direct and response terms [Fig. 1(c)] will be referred to as the pseudopotential pair interaction  $\Phi_{ps}$ . A typical form of  $\Phi_{ps}(r)$  is shown for Ga in Fig. 2,

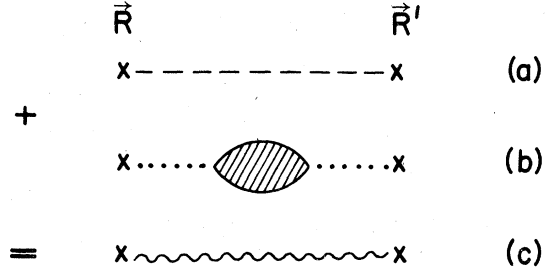


FIG. 1. (a) Direct unscreened Coulomb Interaction (dashed-line) between point ions of charge  $Ze$  at  $\vec{R}$  and  $\vec{R}'$ . (b) Indirect screening contribution via interacting electron gas: Here the polarization insertion corresponds to a pseudopotential coupling (dotted-line) of the ions to the electron gas. (c) The sum of Figs. 1 (a) and (b) resulting in an effective interaction (wiggly-line) between ions at  $\vec{R}$  and  $\vec{R}'$ .

and is obtained by direct Fourier transformation of (16) with an empty-core pseudopotential taken from Ref. 20 and a dielectric function taken from Ref. 24. Note that the energy at the principal minimum is only  $\sim 0.05$  eV or  $\sim 600^\circ\text{K}$ : the effects of screening, as is well known, are considerable. For later use we also observe now that if  $r_c$  is the radius in the empty-core pseudopotential then providing  $r > 2r_c$  (i.e., the ions are separated by greater than an ionic diameter, which is the usual case)  $\Phi_{ps}(r)$  is simply the Fourier transform of

$$(4\pi Z^2 e^2 / q^2) [\cos^2 qr_c / \epsilon(q, 0)], \quad (17)$$

which is nothing more than a screened Coulomb interaction modulated by a simple function reflecting the physical size of the ion in question.

The derivation of (13) yields the lowest-order re-

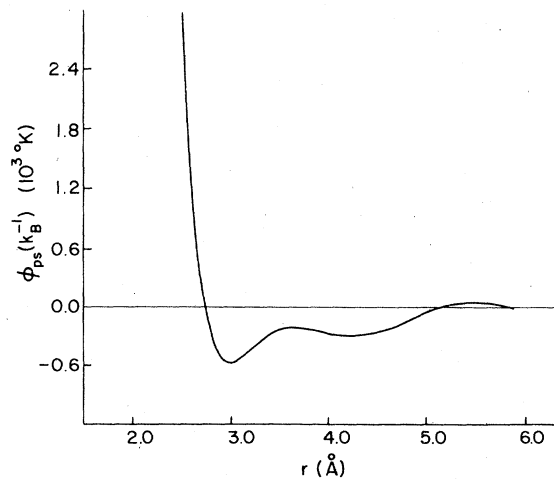


FIG. 2. Pseudopotential pair interaction  $\Phi_{ps}(r)$  for Ga with  $r_c(0) = 1.15a_0$ ,  $q_F = 1.67(a_0^{-1})$  using  $\epsilon_{Hub}$  (see Table 1).

sult that contains (after averaging) the pair distribution function of the ions. Terms arising from nonlinear response can also contribute to effective pairwise interactions.<sup>21</sup> Furthermore, (13) has been written in a form which takes the pseudopotential as local. These are approximations that need not be made in more complete treatments of pseudopotential pair interactions which, however, ignore *direct* coupling between ions resulting in the polarization of the ions themselves. It is this particular aspect that we consider next.

To do so, return to (5) and rewrite it in the form of (6) and (7) (with a thermodynamic limit implied):

$$H = H_0 + H_1,$$

where

$$H_0 = H_v + \sum_{\bar{R}} H_{\bar{R}} + H_M + E_0$$

and

$$H_1 = \sum_{\bar{q} \neq 0} \frac{v_c(q)}{\Omega} \times \left( \frac{1}{2} \sum_{\bar{R}, \bar{R}'} \hat{v}_{\bar{R}}^{\dagger}(\bar{q}) \hat{v}_{\bar{R}'}^{\dagger}(-\bar{q}) + \sum_{\bar{R}} f(q) \hat{v}_{\bar{R}}^{\dagger}(\bar{q}) \hat{\rho}^v(-\bar{q}) + \sum_{\bar{R}, \bar{R}'} Z e^{i\bar{q} \cdot \bar{R}} \hat{v}_{\bar{R}}^{\dagger}(-\bar{q}) + \frac{1}{2} \hat{\rho}^v(\bar{q}) \hat{\rho}^v(-\bar{q}) \right). \quad (18)$$

Here  $f(q) = v_{ps}(q)/Zv_c(q)$ , and, in this notation, the effective static screened interaction between ions at the level of linear response, Eq. (15), is

$$\Phi_{ps}(q, 0) = Z^2 v_c^2(q) \left[ 1 + f^2(q) \left( \frac{1}{\epsilon(q, 0)} - 1 \right) \right]. \quad (19)$$

The point of (18) is that we introduce the pseudopotential at this stage because, as in the rigid-or nonpolarizable-ion treatment, the later intent

is always to regard the valence-electron system as homogeneous. To facilitate identification of terms it is helpful to write

$$H_1 = H_{ii}^{(a)} + H_{ii}^{(b)} + H_{iv} + H_{vv},$$

where

$$H_{ii}^{(a)} = \sum_{\bar{q} \neq 0} \frac{v_c(q)}{\Omega} \frac{1}{2} \sum_{\bar{R}, \bar{R}'} \hat{v}_{\bar{R}}^{\dagger}(\bar{q}) \hat{v}_{\bar{R}'}^{\dagger}(-\bar{q}), \quad (20)$$

$$H_{ii}^{(b)} = \sum_{\bar{q} \neq 0} \frac{v_c(q)}{\Omega} \sum_{\bar{R}, \bar{R}'} Z e^{i\bar{q} \cdot \bar{R}} \hat{v}_{\bar{R}}^{\dagger}(-\bar{q}), \quad (21)$$

$$H_{iv} = \sum_{\bar{q} \neq 0} \frac{v_c(q)}{\Omega} \sum_{\bar{R}} f(q) \hat{v}_{\bar{R}}^{\dagger}(\bar{q}) \hat{\rho}^v(-\bar{q}), \quad (22)$$

and

$$H_{vv} = \sum_{\bar{q} \neq 0} \frac{v_c(q)}{\Omega} \hat{\rho}^v(\bar{q}) \hat{\rho}^v(-\bar{q}). \quad (23)$$

According to (2)  $\hat{v}_{\bar{R}}^{\dagger}(\bar{q})$  is the density-fluctuation operator for the ion at  $\bar{R}$ . Note that  $H_{ii}^{(b)}$  couples this density to the fields due to *point* ions at other locations.

Corresponding to  $H_0$  (all interactions removed) we have a ground state of the form (8), i.e.,

$$\Psi^0 = \Psi_0^v \prod_{\bar{R}} \Phi_{\bar{R}}^0,$$

where  $\Psi_0^v$  is the ground state of a noninteracting electron gas. The energy of  $\Psi^0$  is that of  $NZ$  noninteracting electrons and  $N$  well-separated ions: we will remove these ionic energies from the problem. To obtain the energy of the system in the presence of  $H_1$  we follow the diagrammatic procedure used by Rehr *et al.*<sup>5</sup> If  $H_1(t)$  is an operator in the interaction picture then the  $n$ th-order contribution to the energy is

$$E^{(n)} = \frac{(-i)^{n-1}}{n!} \int_{-\infty}^{\infty} dt_1 \cdots \int_{-\infty}^{\infty} dt_{n-1} \langle \Psi_0 | T H_1(t_1) \cdots H_1(t_{n-1}) | \Psi_0 \rangle_c, \quad (24)$$

where  $T$  is the time-ordering operator and  $c$  designates the fact that only connected diagrams are to be retained order by order. It is easily verified that the first-order contribution from (24) vanishes except for (23). The result is the Madelung energy, the term  $E_0$ , and the Hartree-Fock energy of the uniform electron gas. If, on the other hand, we keep  $H_{ii}$  to first order,  $H_{iv}$  to second order and  $H_{vv}$  to all orders we recover (13).

To obtain contributions from core-polarization terms<sup>4</sup> it is necessary to include  $H_{ii}$  to at least

second order: the simplest such contribution includes  $H_{ii}^{(a)}$  to second order and is shown in Fig. 3. The corresponding energy is

$$E^{(2)} = \frac{i}{2\hbar} \sum_{\bar{q}} \frac{v_c(q)}{\Omega} \sum_{\bar{q}'} \frac{v_c(q')}{\Omega} \sum_{\bar{R} \neq \bar{R}'} \int_{-\infty}^{\infty} dt_1 D_{\bar{R}}(\bar{q}, \bar{q}', t_1) \times D_{\bar{R}'}(-\bar{q}, -\bar{q}', t_1), \quad (25)$$

where

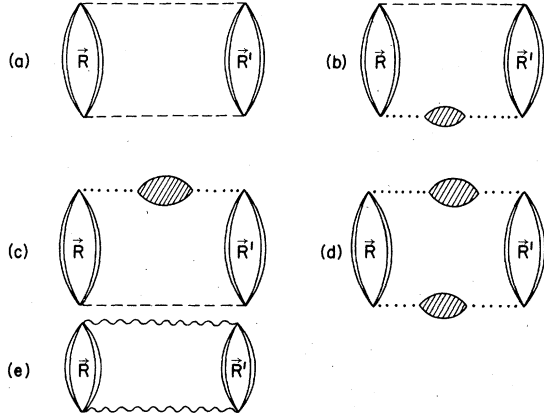


FIG. 3. (a)–(d) Diagrams included in the many-body perturbation calculation outlined in the text. (e) The same diagrams but in terms of an effective interaction (wiggly-line).

$$D_{\vec{R}}(\vec{q}, \vec{q}', t_1) = (-i) \langle \Phi_{\vec{R}}^0 | T \hat{v}_{\vec{R}}^i(\vec{q}) \hat{v}_{\vec{R}}^i(-\vec{q}', t_1) | \Phi_{\vec{R}}^0 \rangle.$$

Equation (25) can also be written

$$E^{(2)} = \frac{i}{2\hbar} \sum_{\vec{q}} \frac{v_c(q)}{\Omega} \sum_{\vec{q}'} \frac{v_c(q')}{\Omega} \sum_{\vec{R} \neq \vec{R}'} \int_{-\infty}^{\infty} \frac{d\omega}{2\pi} D_{\vec{R}}(\vec{q}, \vec{q}', \omega) \times D_{\vec{R}}(-\vec{q}, -\vec{q}', \omega),$$

where

$$D_{\vec{R}}(\vec{q}, \vec{q}', \omega) = (-i) e^{i(\vec{q} - \vec{q}') \cdot \vec{R}} \times \int_{-\infty}^{\infty} dt e^{i\omega t} \langle \Phi_{\vec{R}}^0 | T \left( \vec{q} \cdot \sum_i \vec{r}_{\vec{R},i} \right) \left( \vec{q}' \cdot \sum_i \vec{r}_{\vec{R},i}(t) \right) | \Phi_{\vec{R}}^0 \rangle$$

in the dipole approximation. Since the ions are spherically symmetric on average we have

$$D_{\vec{R}}(\vec{q}, \vec{q}', \omega) = -e^{i(\vec{q} - \vec{q}') \cdot \vec{R}} (\vec{q} \cdot \vec{q}') \frac{2}{3} \sum_n \frac{\omega_{n0} \langle 0 | \sum_i \vec{r}_i | n \rangle^2}{\omega_{n0}^2 - \omega^2},$$

where

$$\hbar\omega_{n0} = \mathcal{G}_{\text{ion}}^n - \mathcal{G}_{\text{ion}}^0$$

and

$$\langle 0 | \sum_i \vec{r}_i | n \rangle = \langle \Phi_{\vec{R}}^0 | \sum_i \vec{r}_i | \Phi_{\vec{R}}^n \rangle.$$

Then,

$$\frac{2}{3} \sum_n \frac{\omega_{n0} \langle 0 | \sum_i \vec{r}_i | n \rangle^2}{\omega_{n0}^2 - \omega^2} = \alpha(\omega),$$

where  $\alpha(\omega)$  is the frequency-dependent ionic polarizability, i.e.,

$$D_{\vec{R}}(\vec{q}, \vec{q}', \omega) = -e^{i(\vec{q} - \vec{q}') \cdot \vec{R}} \alpha(\omega) (\vec{q} \cdot \vec{q}').$$

So the energy becomes

$$E^{(2)} = \frac{i}{2\hbar} \sum_{\vec{q}} \frac{v_c(q)}{\Omega} \sum_{\vec{q}'} \frac{v_c(q')}{\Omega} \times \sum_{\vec{R} \neq \vec{R}'} i \int \frac{d\omega}{2\pi} \alpha^2(\omega) e^{i(\vec{q} - \vec{q}') \cdot (\vec{R} - \vec{R}')} \times (\vec{q} \cdot \vec{q}')^2 = -\frac{N}{2} \sum_{\vec{r}} \int_0^{\infty} \frac{du}{2\pi} \alpha^2(iu) \left[ \left( \frac{\partial^2 v_c(r)}{\partial r^2} \right)^2 + \frac{2}{r^2} \left( \frac{\partial v_c(r)}{\partial r} \right)^2 \right] (\vec{r} \equiv \vec{R} - \vec{R}') \quad (26)$$

which is the sum of  $r^{-6}$  for a pure Coulombic interaction  $v_c(r)$ , as noted by Rehr *et al.*

Next, consider the modifications of (26) arising from the coupling via  $v_{ps}$  of the electrons on the ions to the electron gas the electrons of which are coupled via  $v_c$ . With valence-electron coupling taken, again, to all orders, the first four terms are shown in Fig. 3(b)–3(d): these can be generated by taking Fig. 3(a) and replacing the static screened interaction  $v_c$  by a dynamic interaction  $v(\vec{q}, \omega)$  defined [see (16)] by

$$v(\vec{q}, \omega) = v_c(q) + f^2(q) \Pi(q, \omega), \quad (27)$$

where  $\Pi(q, \omega)$  is the frequency-dependent polarizability of the interacting electron gas. This is displayed in Fig. 3(e). From the structure of Figs. 3(c) and 3(a) and the result Fig. 3(b), we can see immediately that the screened Van der Waals energy can be written

$$E^{(2)} = -\frac{N}{2} \sum_{\vec{r}} \int \frac{du}{2\pi} \alpha^2(iu) \times \left[ \left( \frac{\partial^2 v(r, iu)}{\partial r^2} \right)^2 + \frac{2}{r^2} \left( \frac{\partial v(r, iu)}{\partial r} \right)^2 \right],$$

where

$$v(r, \omega) = \frac{1}{8\pi^3} \int d\vec{q} v(q, \omega) e^{i\vec{q} \cdot \vec{r}}.$$

It follows that we may identify

$$\Phi_{d-d}^s(r) = -\int \frac{du}{2\pi} \alpha^2(iu) \times \left[ \left( \frac{\partial^2 v(r, iu)}{\partial r^2} \right)^2 + \frac{2}{r^2} \left( \frac{\partial v(r, iu)}{\partial r} \right)^2 \right] \quad (28)$$

as the contribution (between ions separated by  $\vec{r}$ ) to their mutual energy from screened fluctuating dipole interactions. The explicit determination of (28) will involve a choice of  $f(q)$ , or more generally its nonlocal equivalent. To demonstrate the major effects we shall simply use an empty-core

form for  $f$  which by an argument identical to the one used in arriving at (17) allows us to write

$$v(q, \omega) = v_c(q) \cos^2[qr_c(\omega)]/\epsilon(q, \omega), \quad (29)$$

where  $\epsilon(q, \omega)$  is the frequency-dependent dielectric function. [In general,  $r_c(\omega \neq 0)$  may be frequency dependent, but is not expected to differ much from the static value. In our numerical evaluation  $r_c(\omega \neq 0)$  is replaced by  $\bar{r}_c$ , a constant value.] Equation (29) is the equivalent of (A8) of Rehr *et al.*<sup>5</sup>; it simply reflects the importance of using a pseudopotential when the valence-electron system is to be regarded as essentially uniform, particularly over the space occupied by the ions themselves.

Before we turn to the form of the *total* pair interaction between ions, we examine the terms arising from  $H_{ii}^{(b)}$  which couple the electrons on one ion with the *static* (monopole) field of another. Evidently only the static polarizability is involved and the lowest-order contributions are shown in Fig. 4(a). Again it is easy to see that the effective interaction [see Fig. 4(d)]

$$v(q) = v_c(q) + f^2(q)\Pi(q, 0)$$

will generate the diagrams 4(b) and 4(c). Thus we arrive at an effective screened monopole-dipole interaction between ions

$$\Phi_{m-d}^s(r) = -Z^2\alpha(0)\left(\frac{\partial v}{\partial \vec{r}}\right) \cdot \left(\frac{\partial v}{\partial \vec{r}}\right)$$

from Fig. 4(d) (i) and an equal and opposite contribution from an ion at  $\vec{R}'$  [Fig. 4(d) (ii)] which has inversion symmetry (with respect to  $\vec{R}'$ ) from  $\vec{R}$ . Thus for a system with inversion symmetry the total contribution from screened monopole-dipole interaction vanishes. When this common symmetry is absent, as for example at a surface, it may be necessary to retain such terms. For the present we assume inversion symmetry. It follows that the total pairwise potential between po-

larizable ions in a simple metal is given by (19) and (28) or for empty-core pseudopotentials in particular,

$$\begin{aligned} \Phi(r) = & \frac{Z^2}{8\pi^3} \int d\vec{q} e^{i\vec{q}\cdot\vec{r}} \frac{v_c(q)}{\epsilon(q, 0)} \cos^2(qr_c) \\ & - \int \frac{du}{2\pi} \alpha^2(iu) \left[ \left( \frac{\partial^2 v(r, iu)}{\partial \vec{r}^2} \right)^2 \right. \\ & \left. + \frac{2}{r^2} \left( \frac{\partial v(r, iu)}{\partial \vec{r}} \right)^2 \right] \quad (30) \end{aligned}$$

with  $v(r, iu)$  given by the Fourier transform (29). Though (30) represents a considerable simplification, particularly through the choice of pseudopotential, it is sufficiently accurate for us to draw a general conclusion concerning the effect of  $f(q)$ . As is well known, the introduction of the pseudopotential into calculations of pair interactions between static ions has a pronounced effect.<sup>3</sup> Here the screened Van der Waals contribution involves dynamic properties of the electron gas rather than static, but the effect of  $f(q)$  is no less pronounced. For example, using representative values of  $\bar{r}_c$ , we find that  $v(r)$  at typical nearest-neighbor separations, can behave as  $a/r^n$ , where  $n \sim 12$ . Thus as a rough estimate, we find for separation  $r$

$$\Phi_{d-d}^s \sim \frac{\alpha^2(0) n^2 [(n+1)^2 + 2]}{6 r^4} v^2(r), \quad (31)$$

where all quantities are measured in atomic units. In very polarizable ions  $\alpha \sim 10$ , and we get  $\Phi_{d-d}^s \sim \Phi_{ps}$  for the case of Ga with  $r \sim 5a_0$  and  $Z = 3$ . The screened fluctuating dipole-dipole interactions can therefore be important.

### III. MODEL EFFECTIVE ION-ION POTENTIALS

For many simple metals it is an excellent approximation to neglect the second term of (30) when considering the effective pair potential between ions. Roughly speaking we can expect the justification of this to hinge on the polarizability of the ion being small though as we shall see one has to apply this argument with caution because of the derivative nature in the terms appearing in the screened fluctuating dipole-dipole interaction [see (31)]. We shall now turn to the way in which the valence electrons enter the problem beginning with the frequency-dependent response required in (29). It is clear that frequencies not too distant from the plasma frequency  $\omega_p$  of the electron gas will be important: if the ions are so tightly bound that their relevant frequencies are greatly in excess of  $\omega_p$ , then screening effects are unimportant and the second term of (30) will lead to the standard London force.

The simplest (Lindhard<sup>22</sup>) form for  $\epsilon(q, \omega)$  re-

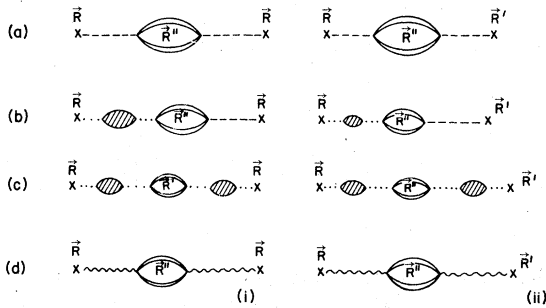


FIG. 4. (a)-(c) Diagrams which contribute to the monopole-dipole forces. (i) For the two-body monopole-dipole-monopole interaction. (ii) For the three-body monopole-dipole-monopole interaction.

sults from the random-phase approximation (RPA), but suffers from the neglect of exchange and correlation effects which we find to be as important in this problem as they are in their influence on the pseudopotential pair interaction.<sup>19</sup> To include them properly is a difficult undertaking and we have followed a route suggested by Langreth,<sup>23</sup> namely, to write

$$1 - \frac{1}{\epsilon(q, \omega)} = \frac{\Pi_0(q, \omega)}{1 + [1 - G(q, \omega)]\Pi_0(q, \omega)} \quad (32)$$

(where  $\Pi_0$  is the Lindhard polarizability) with  $G(q, \omega)$  representing an approximation for exchange and correlation effects (see Table I). The form of (32) is identical to that obtained by Hubbard<sup>24</sup> in summing a restricted set of diagrams arising in the perturbation calculation of the polarization. In this calculation, and in others of a similar spirit, the correction for exchange and correlation is static. Truly dynamic corrections have been proposed by Kleinman,<sup>25</sup> Overhauser,<sup>26</sup> and Langreth<sup>23</sup>; in Langreth's calculation the choice of exchange and correlation correction is guided by

TABLE I. Electron dielectric function, Eq. (32).

$\epsilon$	$G$
$\epsilon_{\text{Hub}}$	$G = \frac{1}{2} \left( \frac{y^2}{y^2 + \frac{1}{2}(1 + 0.158/\pi q_F a_0)} \right)^{-1}$
$\epsilon_{\text{KL}}$	Eq. (33)
$\epsilon_{\text{TW}}$	Table given in Ref. 28
$\epsilon_{\text{RPA}}$	$G = 0$

the use of a variational principle. A reasonable approximation for  $q \geq 2q_F$  can be shown to be

$$G(q, iu) = \frac{1}{4} \left( \frac{1 + F^2}{1 + D} + \frac{1 - F^2}{D} \right), \quad (33)$$

where

$$F = x \left[ 1 + \frac{y}{2} \ln \left| \frac{(1-y)^2 + x^2}{(1+y)^2 + x^2} \right| - \frac{1}{2} \left( x + \frac{1}{x} - y \right) \tan^{-1} \left( \frac{2x}{x^2 + y^2 - 1} \right) \right] / \left[ -1 + \frac{1}{4y} (1 - y^2 + x^2) \ln \left| \frac{(1-y)^2 + x^2}{(1+y)^2 + x^2} \right| + x \tan^{-1} \left( \frac{2x}{x^2 + y^2 - 1} \right) \right],$$

and

$$D = 1 + \frac{1}{2y^2} \frac{1}{(1 + 0.158/\pi a_0 q_F)},$$

with  $y = q/2q_F$  and  $x = \hbar u/4y\epsilon_F$ .

It is important to note that although the derivation of (33) preserves certain symmetry constraints,<sup>23</sup> it is nevertheless an approximation. Since an exact expression for  $\epsilon(q, \omega)$  is lacking, it is not possible for us to judge the relative merit of (33) versus other approximations,<sup>27-29</sup> such as that of Toigo and Woodruff<sup>28</sup> (which is also static). On the other hand, it is worth emphasizing that the essential aspects of screening of the fluctuating dipole forces appears to be present when any of the various approximations for  $G$  is used. It is only a matter of degree to which these effects are ultimately manifested in the resulting effective pair interaction: the results we shall present are based both on Eq. (33) (which at least attempts to go beyond the static approximation for exchange and correlation effects) and on various other static approximations.

To investigate the dependence of the screened fluctuating dipole contribution on electron density (which governs, for example, the plasma frequency), the pseudopotential (represented here as an empty-core form), and exchange and correlation correction, we have rewritten (28) as

$$\Phi_{d-d}^s(r) = \int_0^\infty \frac{du}{2\pi} \alpha^2(iu) F(iu),$$

where

$$F = \left( \frac{\partial^2 v(r, iu)}{\partial r^2} \right)^2 + \frac{2}{r^2} \left( \frac{\partial v(r, iu)}{\partial r} \right)^2,$$

in which, according to (29)

$$v(r, iu) = \int \frac{d\vec{q}}{(2\pi)^3} e^{i\vec{q} \cdot \vec{r}} \frac{4\pi e^2}{q^2} \frac{\cos^2(q\vec{r}_c)}{\epsilon(q, iu)} \quad (r > 2r_c). \quad (34)$$

The form factor

$$F = F(iu, \vec{r}_c, q_F, G)$$



has been determined for Ga, Na, and Rb by direct numerical Fourier transformation. Values of  $\bar{r}_c$  have been taken from the literature.<sup>7</sup> Some typical results are shown in Figs. 5-7. In what follows we shall be concentrating mainly on the form of  $\Phi_{d-d}^s$  at short separation since this is the region of physical relevance in the determination of structure.

One striking result that emerges is the sensitivity of the small-separation behavior of  $F$  to the presence of  $f(q)$ , the pseudopotential. Though this has been approximated by an empty-core potential, the behavior can be expected to be general in the same sense that the pseudopotential has an important bearing on the screened pair interaction  $\Phi_{ps}$ . The degree to which  $F$  is dependent on  $\bar{r}_c$  can be seen in Fig. 5 where the vanishing of  $\bar{r}_c$  produces very significant changes in the form factor, particularly at low frequencies ( $u \lesssim \omega_p$ ). These changes are progressively reduced as fre-

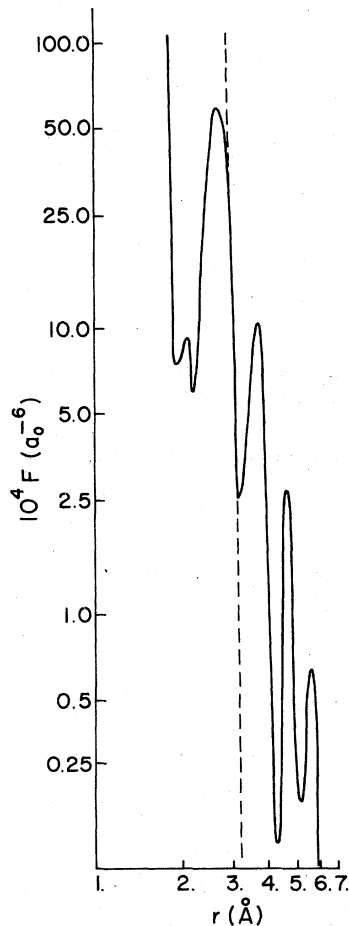


FIG. 5. Form factors  $F$  [see Eq. (34)] for Ga at  $q_f = 0.885 (a_0^{-1})$ ,  $u = 0$  and using  $\epsilon_{\text{Hub}}$  (see Table I); Solid-line,  $\bar{r}_c(0) = 0$ ; dashed-line,  $\bar{r}_c(0) = 1.25 a_0$ .

quency increases becoming rather small at  $u \sim 2\omega_p$ . This is to be expected: at high frequency  $\epsilon(q, \omega)$  approaches unity and the form factor assumes an  $r^{-6}$  form typical of unscreened fluctuating dipole forces. Note that the oscillations in  $F$  at large separation are the analog of the Friedel oscillations in the pseudopotential pair interaction. They have the same origin, namely, the sharpness of the Fermi surface, and will presumably also be damped at finite temperatures.

From the calculations of  $F$  we also learn that it is rather insensitive to  $q_f$  (a change of less than 10% is typical for  $r < 2.6 \text{ \AA}$  when  $q_f$  changes by 10%). On the other hand the "steepness" of  $F$  at nearest-neighbor distances can change rather significantly as the pseudopotential changes. This is of some interest when we compare alkali metals (large  $\bar{r}_c$ , Fig. 6) with polyvalent metals (small  $\bar{r}_c$ , Fig. 7). This "steepness" appears to be enhanced by small values of  $\bar{r}_c$ ; it is weakly dependent on  $q_f$ . We shall see shortly that this feature of the screened fluctuating dipole contribution to the pair potential manifests itself in a different

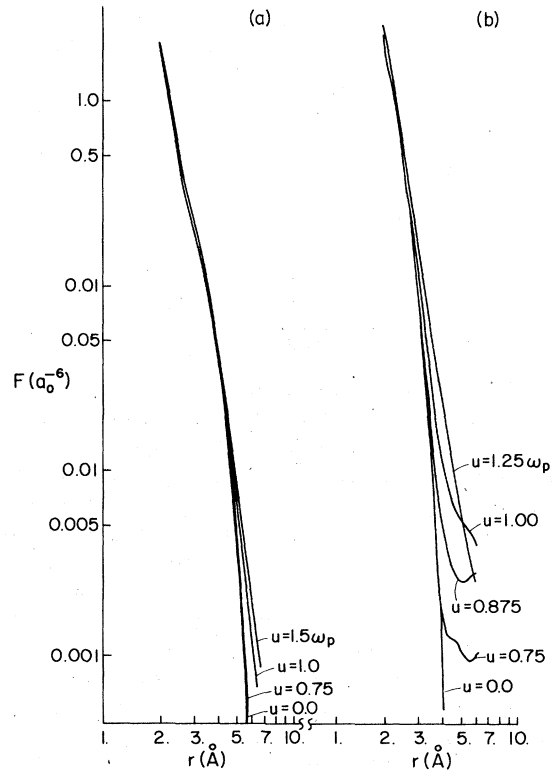


FIG. 6. (a) Form factors for Rb at  $q_f = 0.358 (a_0^{-1})$ ,  $\bar{r}_c(0) = 2.716 a_0$ ,  $u = (0, 0.75, 1.0, 1.5)\omega_p$  ( $\omega_p$  is the electron-plasma frequency) using  $\epsilon_{\text{Hub}}$  (see Table I). (b) Form factors for Na at  $q_f = 0.47 (a_0^{-1})$ ,  $\bar{r}_c(0) = 1.66 a_0$ ,  $u = (0, 0.75, 0.875, 1.0, 1.25)\omega_p$  using  $\epsilon_{\text{Hub}}$  (see Table I).

fashion in the two classes of metals.

Figure 7 shows the sensitivity of  $F$  to different choices of the response function, all calculated for the same  $\bar{r}_c$  and  $q_F(u=0)$ . The response functions used are those discussed above; i.e., taken from Toigo and Woodruff<sup>23</sup> (TW), Hubbard,<sup>24</sup> and RPA<sup>22</sup> (all static exchange and correlation corrections) and Kleinman and Langreth<sup>25</sup> (KL) (dynamic). Note that the form factors coincide at small separation, and although they are qualitatively similar at large separation there are quantitative differences that can affect the ultimate shape of the effective ion-ion interaction.

To obtain the ion-ion interactions themselves, we also need the frequency-dependent polarizabilities  $\alpha(\omega)$  for the ions. Though these can be calculated in principle,<sup>30</sup> and also can be measured<sup>31,5</sup> over a large (but necessarily limited) range of frequencies, we have adopted a Lorentzian form

$$\alpha(iu) = \alpha_0 / [1 + (u/u_0)^2], \quad (35)$$

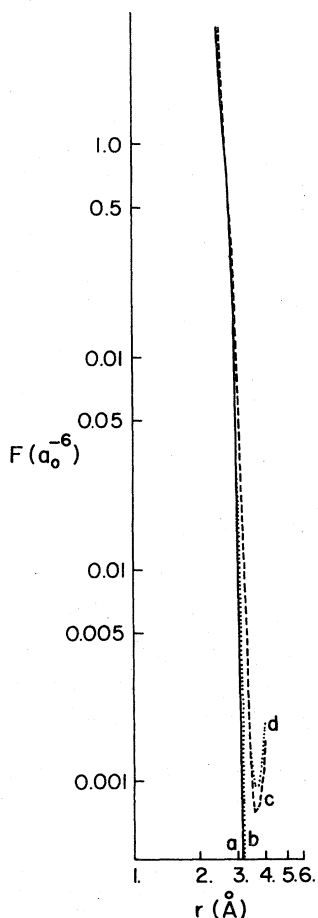


FIG. 7. Form factors for Ga at  $q_F = 0.885 (a_0^{-1})$ ,  $\bar{r}_c(0) = 1.66a_0$ ,  $u=0$  for (a)  $\epsilon_{KL}$ , (b)  $\epsilon_{Hub}$ , (c)  $\epsilon_{TW}$ , (d)  $\epsilon_{RPA}$  (see Table I).

where  $\alpha_0$  is the static polarizability and is available for many metallic ions.<sup>31</sup> The parameter  $u_0$ , a measure of the binding of the electron in the ion, can be adjusted to the low-frequency dependence of the polarizability. Such a value of  $u_0$  will not, of course guarantee that the sum rule satisfied by the physical  $\alpha(\omega)$  will be satisfied. As it happens, however, the conclusions we shall draw next do not depend very seriously on the choice of  $u_0$ . With these remarks in mind, we have calculated

$$\Phi_{d-d}^s(r) = -\frac{1}{2\pi} \int du \alpha^2(iu) F(iu, \bar{r}_c, q_F, G), \quad (36)$$

with  $\alpha$  given by (35), and the screened pseudopotential pair interaction from

$$\Phi_{ps}(r) = \frac{Z^2}{8\pi^3} \int d\vec{q} e^{i\vec{q} \cdot \vec{r}} \frac{v_c(q)}{\epsilon(q, 0)} \cos^2(qr_c). \quad (37)$$

The Fourier transforms required here are performed numerically with values of  $r_c$  again taken from the literature.<sup>7</sup> As noted earlier the sum  $\Phi_{d-d}^s + \Phi_{ps}$  must be augmented at very short range (separations on the order of an ionic diameter) by the core-core exchange repulsion which for our purposes can be sufficiently well approximated by a simple Born-Mayer form  $\Phi_{BM}(r) = A e^{-Br}$ .

It is possible to find in the literature a range of values for  $A$  and  $B$  depending on the system of interest. The values quoted very often also depend,

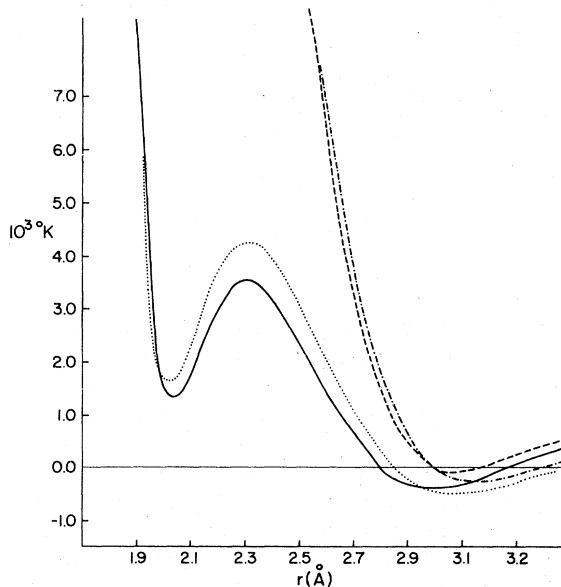


FIG. 8. Effective ion-ion potential for Ga,  $q_F = 0.885 (a_0^{-1})$ ,  $\bar{r}_c = 1.25a_0$ ,  $r_c(0) = 1.43a_0$ ,  $\alpha_0 = 1.7 \text{ \AA}^3$ ,  $u_0 = 10 \text{ eV}$ ,  $A = 5.67 \times 10^{11} \text{ K}$ ,  $B = 8.5 (\text{ \AA}^{-1})$ . Solid-line,  $\epsilon_{KL}$ ; dotted-line,  $\epsilon_{Hub}$  (see Table I).  $\Phi_{ps}(r)$ ;  $r_c(0) = 1.43a_0$ , dashed-line,  $\epsilon_{KL}$ ; dash-dotted line,  $\epsilon_{Hub}$ .

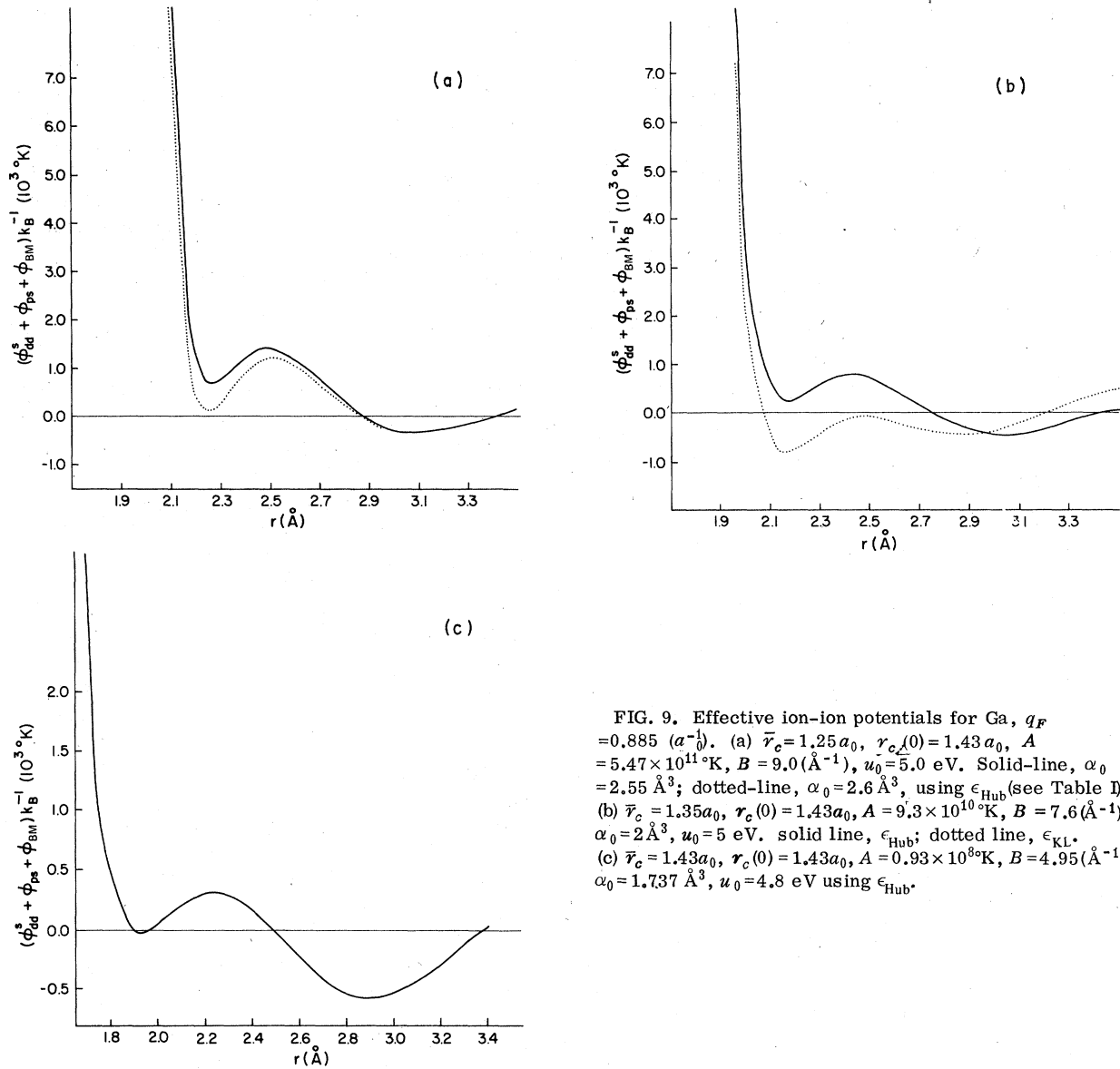


FIG. 9. Effective ion-ion potentials for Ga,  $q_F = 0.885 (a_0^{-1})$ . (a)  $\bar{r}_c = 1.25 a_0$ ,  $r_c(0) = 1.43 a_0$ ,  $A = 5.47 \times 10^{11} \text{K}$ ,  $B = 9.0 (\text{\AA}^{-1})$ ,  $u_0 = 5.0 \text{ eV}$ . Solid-line,  $\alpha_0 = 2.55 \text{\AA}^3$ ; dotted-line,  $\alpha_0 = 2.6 \text{\AA}^3$ , using  $\epsilon_{\text{Hub}}$  (see Table I). (b)  $\bar{r}_c = 1.35 a_0$ ,  $r_c(0) = 1.43 a_0$ ,  $A = 9.3 \times 10^{10} \text{K}$ ,  $B = 7.6 (\text{\AA}^{-1})$ ,  $\alpha_0 = 2 \text{\AA}^3$ ,  $u_0 = 5 \text{ eV}$ . solid line,  $\epsilon_{\text{Hub}}$ ; dotted line,  $\epsilon_{\text{KL}}$ . (c)  $\bar{r}_c = 1.43 a_0$ ,  $r_c(0) = 1.43 a_0$ ,  $A = 0.93 \times 10^8 \text{K}$ ,  $B = 4.95 (\text{\AA}^{-1})$ ,  $\alpha_0 = 1.737 \text{\AA}^3$ ,  $u_0 = 4.8 \text{ eV}$  using  $\epsilon_{\text{Hub}}$ .

for a given system, on the nature of the electron states chosen. For example, in the case of Cu, a recent Hartree-Fock calculation<sup>32</sup> which uses ionic wave functions appropriate to the neutral atom, does not agree with a more extensive variational calculation for a true ion.<sup>33</sup> This indicates that the orbitals used in the latter may be more extensive than those taken from a neutral-atom calculation. As it turns out the results we present reflect more the longer-ranged part of the potential, and though the short-range cutoff is necessary, as discussed above, the values attached to  $A$  and  $B$  do not influence the calculations significantly (the values quoted in the captions to Figs. 8 and 9 show a typical range of variation). For the alkali

metals the Born-Mayer repulsion term is exceedingly small for inter-ion separations typical of normal liquid and solid densities. In some of the polyvalent metals (e.g., Ga) the Born-Mayer repulsion term might become significant at reasonable compression.

We have calculated the effective ion-ion interaction<sup>4</sup>

$$\Phi_{\text{eff}}(r) = \Phi_{\text{BM}}(r) + \Phi_{d-d}^s(r) + \Phi_{\text{ps}}(r)$$

for Ga, Na, and Rb for a reasonable range of parameters appearing in (30) and for different choices of dielectric function (see Figs. 8-13). From the results it appears to be the case that for ions with high polarizability the screened fluc-

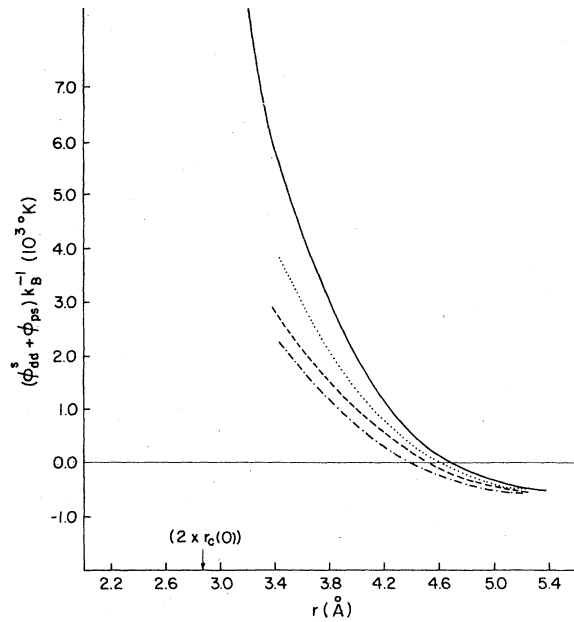


FIG. 10. Effective ion-ion potential for Rb using  $\epsilon_{\text{Hub}}$  (see Table I),  $q_F = 0.358(a_0^{-1})$ .  $\Phi_{d-d}^s + \Phi_{ps}$  ( $\Phi_{BM}$  is very small in this region of separation). Dotted line,  $\bar{r}_c = 2.5a_0$ ,  $r_c(0) = 2.716a_0$ ,  $u_0 = 5$  eV,  $\alpha_0 = 1.7 \text{ \AA}^3$ ; dashed line,  $\bar{r}_c = 2.5a_0$ ,  $r_c(0) = 2.716a_0$ ,  $u_0 = 15$  eV,  $\alpha_0 = 1.7 \text{ \AA}^3$ ; dash-dotted line,  $\bar{r}_c = 2.716a_0$ ,  $r_c(0) = 2.716a_0$ ,  $u_0 = 30$  eV,  $\alpha_0 = 1.7 \text{ \AA}^3$ ; solid line,  $\Phi_{ps}$ ,  $r_c(0) = 2.716a_0$ .

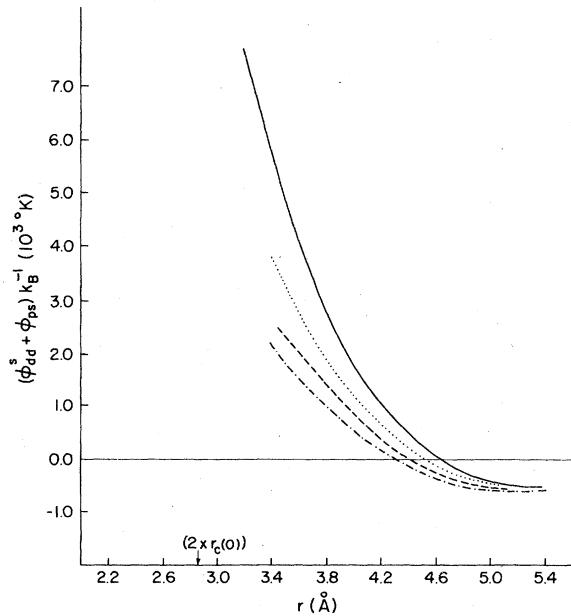


FIG. 11. Same as in Fig. 10 except that  $\epsilon_{\text{KL}}$  is used (see Table I).

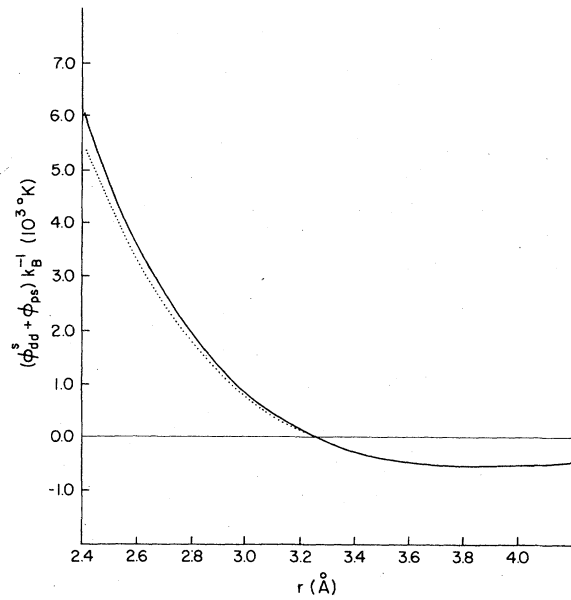


FIG. 12. Effective ion-ion potential for Na using  $\epsilon_{\text{Hub}}$  (see Table I),  $q_F = 0.474(a_0^{-1})$ ,  $\Phi_{d-d}^s + \Phi_{ps}$  ( $\Phi_{BM}$  is very small in this region of separation). Dotted line,  $\bar{r}_c = 1.66a_0$ ,  $r_c(0) = 1.66a_0$ ,  $u_0 = 30$  eV,  $\alpha_0 = 0.2 \text{ \AA}^3$ ; solid line,  $\Phi_{ps}$ ,  $r_c(0) = 1.66a_0$ .

tuating dipole interaction has an important influence on the repulsive part of  $\Phi_{ps}$ . This influence can range from a "softening" of the short-range part of the effective ion-ion interaction in

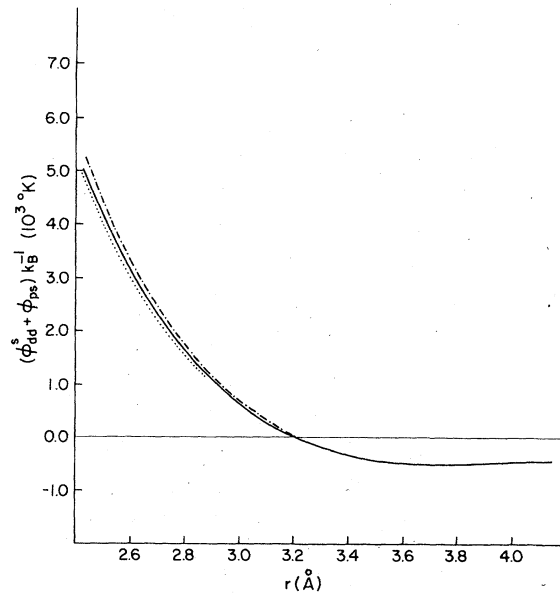


FIG. 13. Same as Fig. 12 except that  $\epsilon_{\text{KL}}$  is used (see Table I). Solid line,  $\bar{r}_c = 1.46a_0$ ,  $u_0 = 15$  eV; dotted line,  $r_c = 1.66a_0$ ,  $u_0 = 30$  eV; dash-dotted line,  $\Phi_{ps}$ ,  $r_c(0) = 1.66a_0$ .

monovalent metals such as Rb (Figs. 10 and 11), to the formation of a secondary minimum in polyvalent metals such as Ga (see Fig. 8 and 9). The detailed shape of  $\Phi_{\text{eff}}$  reflects the choice of the exchange-correlation correction used in  $\epsilon(q, \omega)$ . But the essential factor in obtaining a secondary minimum is that the screened fluctuating dipole interactions be sufficiently large yet be a rapid function of separation. These conditions are most likely to be met in polyvalent simple metals with highly polarizable yet compact ions (i.e., with rather small  $r_c$  and large  $q_F$ ). The characteristic nearest-neighbor separations in the alkali metals is such that the contribution from  $\Phi_{d-d}^s$  tends rather to lead to a general softening of  $\Phi_{\text{eff}}$ . This is consistent with the interpretation by Page *et al.*<sup>17</sup> on the inferences that can be drawn on  $\Phi_{\text{eff}}$  from the structure of liquid Rb (see Sec. I).

A subsidiary minimum in  $\Phi_{\text{eff}}$  ought to have structural consequences provided it is within reach of typical thermal energies. We will consider this prospect in more detail in a moment, but for the present an inspection of Table II shows that it may not be fortuitous that those liquid simple metals exhibiting anomalies in their static structure factors  $S(k)$  are polyvalent metals whose ions con-

TABLE II. Parameters for the ions of the simple metals. Here  $Z$  is the valence,  $m$  the number of electrons in the outer shell of the ion,  $r_c$  is the empty core radius used in Eq. (17), and  $\alpha_0$  is the static polarizability. Also tabulated is the excess entropy of melting per ion,  $S_E/Nk_B$ .

	$Z$	$m^a$	$r_c$ ( $\text{\AA}$ ) <sup>b</sup>	$\alpha_0$ ( $\text{\AA}^3$ ) <sup>c</sup>	$S_E/Nk_B$ <sup>e</sup>
Li <sup>+</sup>	1	2	0.56	0.0286	3.7
Na <sup>+</sup>	1	6	0.88	0.2	3.55
K <sup>+</sup>	1	6	1.115	0.9	3.61
Rb <sup>+</sup>	1	6	1.5	1.7	
Cu <sup>+</sup>	1	10	0.93	1.7 <sup>(5)</sup>	3.6
Hg <sup>2+</sup>	2	10	0.484	2.78	5.1
Zn <sup>2+</sup>	2	10	0.673	0.8	
Cd <sup>2+</sup>	2	10		1.8	4.15
Al <sup>3+</sup>	3	6	0.59	0.053	3.6
Ga <sup>3+</sup>	3	10	0.608	~1.7 <sup>f</sup>	4.75
In <sup>3+</sup>	3	10	0.7	0.729 <sup>d</sup>	4.4
Si <sup>4+</sup>	4	6		0.04	(2.5)
Ge <sup>4+</sup>	4	10		1.0	(1.0)
Sn <sup>4+</sup>	4	10	0.686	3.4	4.2
Pb <sup>4+</sup>	4	10	0.78	0.6 <sup>d</sup>	4.1
Sb <sup>5+</sup>	5	10		0.36 <sup>d</sup>	3.2
Bi <sup>5+</sup>	5	10	0.79	0.45 <sup>d</sup>	3.9

<sup>a</sup>Number of electrons in the outer shell.

<sup>b</sup>Estimate of empty-core radius taken from Ref. 7.

Note: such estimates are not unique.

<sup>c</sup>Experimental values from Ref. 31.

<sup>d</sup>Estimates from Ref. 44.

<sup>e</sup>Estimates listed in Ref. 45.

<sup>f</sup>Estimated to be close to Cu<sup>+</sup>, which is more reliable than Zn<sup>2+</sup>.

tain a filled (10-electron)  $d$  shell. The large number of outer ionic-electrons leads to a relatively high polarizability and the polyvalency ensures a large Fermi momentum and a small  $r_c$ . In principle the primary minimum and secondary minimum in  $\Phi_{\text{eff}}$  will define two characteristic distances which in turn may emerge in  $S(k)$ . That they in fact do has to be established by direct calculation for it is known that features in a pair potential at distances *greater* than the principal minimum generally have little effect on the  $S(k)$  of dense simple liquids. Section IV is therefore devoted to a discussion of a series of Monte Carlo calculations of  $S(k)$  for a model system interacting with a model potential containing the major features of  $\Phi_{\text{eff}}$ .

These calculations will show that the anomalies in  $S(k)$  can be attributed to screened fluctuating dipole interactions. It is worth remarking here that simulation studies on the alkali metals have already been performed and a calculation<sup>34</sup> of  $S(k)$  for liquid Na utilizing a Lennard-Jones-like potential has been shown to agree quite well with the measured  $S(k)$ . On the other hand a recent simulation<sup>35</sup> on Rb leads to a conclusion that a short-range potential softer than  $r^{-12}$  will give better agreement with experiment. This is consistent with our calculations on Rb: for  $u_0 \sim 30$  eV and  $\alpha_0 = 11.48(\text{\AA}^3)$  we find a repulsive core resembling much more an  $r^{-10}$  behavior. In contrast to this, the calculations in Na [for which  $\alpha_0 \sim 1.35(\text{\AA}^3)$ ] confirm a rather hard core resembling  $r^{-12}$ . We should remark though, that recent simulation studies<sup>34</sup> on liquid Na appear to be somewhat in conflict with the reported agreement of the measured  $S(k)$  with other machine studies carried out near melting of a system interacting via  $r^{-4}$ -type potentials.

Finally it should be noted that the point we have made concerning the importance of core-polarization effects will be relevant to certain alloy systems in which one or more constituents possesses highly polarizable ions. In an alloy, the Fermi wave vector can change with concentration and the relative weights of screened pseudopotential and core-polarization effects will likewise change. Before these are investigated systematically however, it may be necessary to understand in more depth the dynamics of the interacting electron gas which enter, as we have noted, in the rather poorly known exchange and correlation corrections to  $\epsilon(q, \omega)$ .

#### IV. MONTE CARLO CALCULATIONS FOR MODEL SYSTEMS

We now discuss the results of a series of Monte Carlo calculations carried out for two model liquid

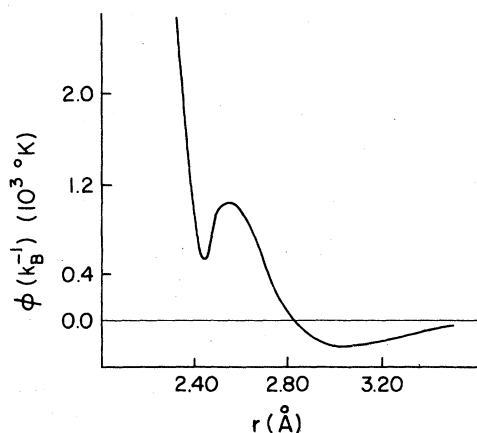


FIG. 14. A model potential used in the Monte Carlo simulation of liquid Ga.

systems in which the particles interact with different pair potentials. Both of these potentials display a secondary minimum at small separation attributable to core-polarization effects [see Figs. 10(c) and 14]. We have used the Monte Carlo method<sup>36</sup> to obtain the structure factor  $S(k)$  by directly evaluating

$$S(k) = \langle Q_{\vec{k}}^* Q_{-\vec{k}} \rangle, \quad (38)$$

with

$$Q_{\vec{k}} = \frac{1}{\sqrt{N}} \sum_{j=1}^N \exp(i\vec{k} \cdot \vec{R}_j), \quad (\vec{k} \neq 0).$$

The canonical ensemble averages implied in (38) are over the configurations generated by the Monte Carlo procedure. Here  $N$  is the number of particles (up to 400) which are taken as confined in a cubic box to which the standard periodic boundary conditions are appended [the  $S(k)$  is therefore evaluated at reciprocal-lattice vectors ( $\vec{K}$ )]. Markov chains containing up to  $1.9 \times 10^6$  configurations were used in order to ensure adequate convergence. The pair correlation function  $g(r)$  can also be evaluated directly by recording the normalized probability of finding pairs separated by  $r$  averaged over the Markov chain.

We have tested this Monte Carlo procedure extensively by performing calculations with systems in which the particles interact with standard potentials not displaying the short-range secondary minimum. The results for both  $S(k)$  and  $g(r)$  are in good agreement with published results. In addition we have performed a series of simulation studies in which the interaction between particles is taken as  $\Phi_{ps}(r)$  alone (the pair potential based on the pseudopotential formalism). For the case of liquid Ga [see Figs. 2, 15(a), and 15(b)] we obtain results that are quite typical of simple liquids, for both  $S(k)$  and  $g(r)$ . This seems to be a clear indication that the structural anomalies cannot be ac-

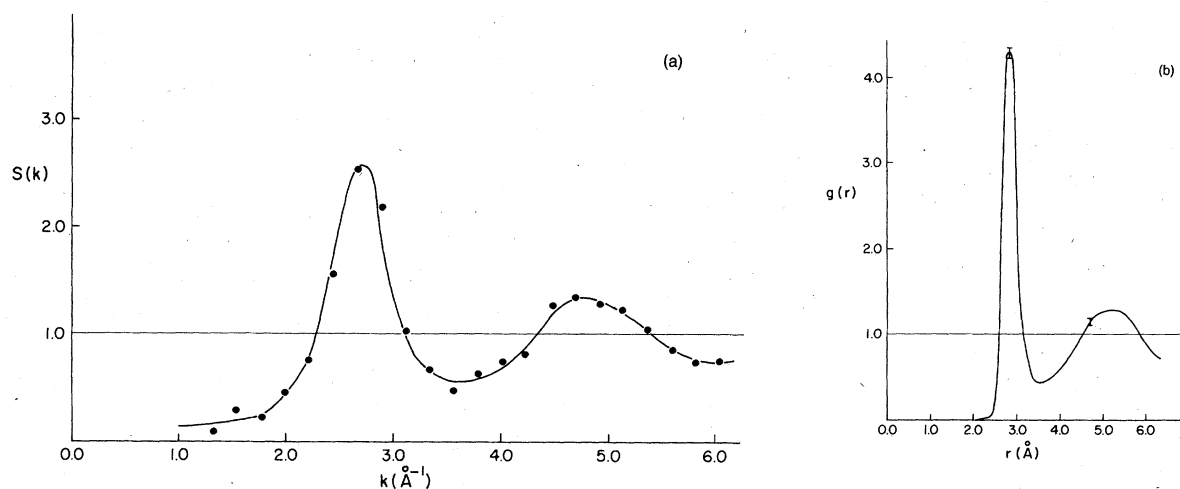


FIG. 15. (a)  $S(k)$  calculated with the potential of Fig. 2 (no core-polarization effects) using 145 particles. Here  $T = 296^\circ\text{K}$  and the density is  $0.0528 \text{ (\AA}^{-3}\text{)}$ . (b)  $g(r)$  calculated with the potential of Fig. 2 ( $T = 296^\circ\text{K}$ ).

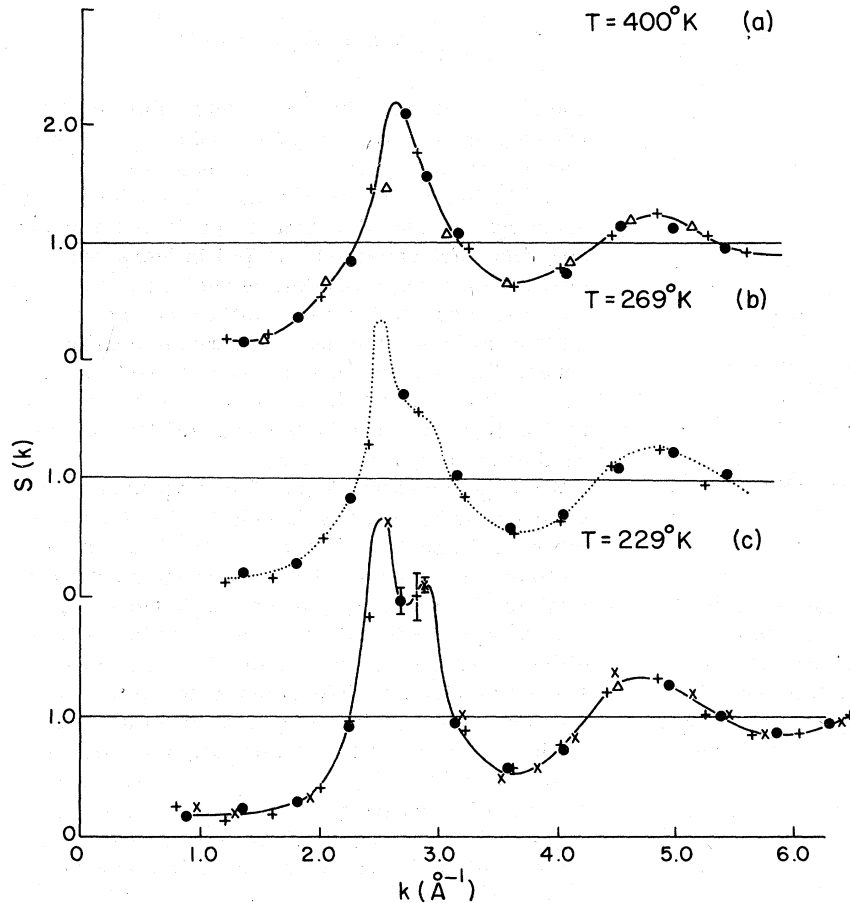


FIG. 16.  $S(k)$  calculated with the potential of Fig. 14. (a) At a temperature  $T = 400^\circ\text{K}$ . Here,  $+$   $\equiv$  200,  $\bullet$   $\equiv$  145, and  $\Delta$   $\equiv$  100 particles. (b) At a temperature  $T = 269^\circ\text{K}$ . Here,  $+$   $\equiv$  200 and  $\bullet$   $\equiv$  145 particles. (c) At a temperature  $T = 229^\circ\text{K}$ . Here  $*$   $\equiv$  400,  $+$   $\equiv$  200 and  $\bullet$   $\equiv$  145 particles.

counted for within standard pair force models, but require the inclusion of forces with a different physical origin. The calculations we now describe have been carried out to test the proposition that the structural anomalies are directly related to the core-polarization contributions to the potentials. They have been carried through in two stages. First we performed a series of exploratory simulations on systems in which the characteristic features of the pair potentials (e.g., position of subsidiary minima, characteristic barrier heights, etc.) were systematically varied in order to understand the consequent effects on the resulting structure factors. From these studies we are able to conclude that the proposition just described is fundamentally correct. For further analysis we therefore adopted a single model potential to represent liquid gallium; the secondary minimum occurs at  $2.4 \text{ \AA}$ , as shown in Fig. 14. For this choice we calculated both  $S(k)$  and  $g(r)$  at a number density of  $0.0528 \text{ \AA}^{-3}$  (and using up to 400 particles in order to check the size dependence of the procedure). The results of this series of calculations are shown in Figs. 16–19. The most prominent result is the

appearance of the “structural anomaly” on the peak of  $S(k)$  which is qualitatively similar to the experimental observation. (See Figs. 20 and 21.) A comparison between our calculated structure factor and the experimental curve, particularly with respect to the location of the subsidiary maximum leads us to conclude that the model potential used is likely to embody the essential physical features of the actual effective pair potential between gallium ions. Inspection of the effective ion-ion interactions that we have actually calculated (Sec. III) reveals that one such prominent feature, the appearance of nonmonotonic behavior in the pair potential, can be obtained over a rather wide range of parameters.

We have also calculated using the potential of Fig. 14, the pair distribution function  $g(r)$  for liquid Ga. It displays a striking bimodal distribution [see Figs. 19(a)–(c)] reflecting the fact that the secondary minimum is a preferred region for particle localization. On account of the magnitude of the potential barrier separating the two minima in the potential, small changes in temperature have relatively minor effect on the structure re-

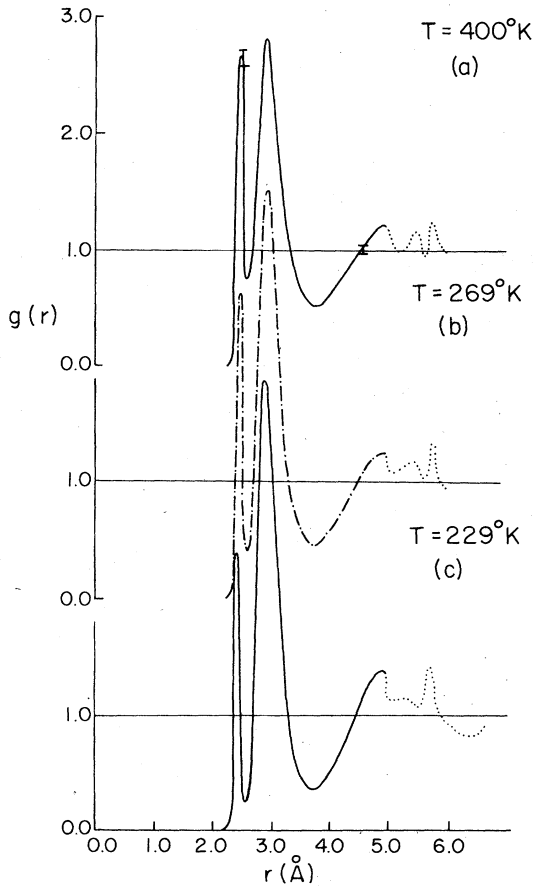


FIG. 17.  $g(r)$  calculated with the potential of Figure 14 at (a)  $T=400^\circ\text{K}$ , (b)  $T=269^\circ\text{K}$ , (c)  $T=229^\circ\text{K}$ . Vertical bars denote typical estimated errors.

flected either in  $g(r)$  or in  $S(k)$  [see for example Figs. 20 and 16(c) for a temperature of  $229^\circ\text{K}$ ]. As temperature increases, however, the potential barrier becomes progressively more surmountable and it becomes more probable for pairs of ions to occupy the higher-energy minima [see Figs. 17(a)–17(c)]. At very high temperatures ( $k_B T \gg$  barrier height) only the inner repulsive part of the potential is physically important and the structure approaches that of a simple liquid. The diminishing character of the anomaly in  $S(k)$  at  $400^\circ\text{K}$  [Fig. 16(a)] is thus to be expected. On the other hand, structure in  $g(r)$  still persists [Fig. 17(c)] which provides yet another example of the fact that  $S(k)$  is relatively insensitive to the details of pair interaction.

In the second stage of our Monte Carlo calculations we have examined a system in which the model pair potential displays a minimum at  $1.9 \text{ \AA}$  (see Fig. 9), the parameters otherwise being appropriate to Ga. We have simulated both  $S(k)$

and  $g(r)$  at three different temperatures, but again at a fixed number density of  $0.0528 \text{ \AA}^{-3}$ . The results (at  $T=323, 373,$  and  $423^\circ\text{K}$ ) are given in Figs. 18 and 19 and may be compared with the experimental data given in Figs. 20 and 21. The data, it will be noted, are for  $T=233$  and  $296^\circ\text{K}$ : the point is that reducing the temperature below the values cited above for the simulations leads to states which cannot be guaranteed to represent liquids. In this respect, the structure in the potential is quite important.

The calculations show that much can be inferred about the detailed form of the pair potentials in this class of metals by systematic analysis and matching of the  $S(k)$  determined from experiment over a range of temperatures with the  $S(k)$  obtained from machine calculations. As noted earlier the precise form of  $S(k)$  clearly depends on the nonmonotonic part of the potential, and this, in turn, has a nontrivial dependence on ion-core polarizability, and electron-gas dielectric functions.

We end this section by comparing the results obtained here with those from other calculations addressing the problems of anomalies in  $S(k)$ . Integral equation studies<sup>37</sup> of systems interacting with potentials of the form

$$\Phi(r) = \Phi_{\text{HS}}(r) + (A/r)e^{\xi r}$$

[where  $\Phi_{\text{HS}}(r)$  is a hard-sphere potential] report a structure factor with a distinct subsidiary maximum. Similarly, for step potentials<sup>38</sup> of the type

$$\Phi(r) = 0, \quad r > \lambda\sigma$$

$$\Phi(r) = \epsilon, \quad \sigma < r < \lambda\sigma$$

$$\Phi(r) = \infty, \quad r < \sigma$$

results from both Monte Carlo simulation<sup>39</sup> and calculations based on the random-phase approximation also show subsidiary maxima in  $S(k)$ . Since the potentials we propose are characterized in part by two length scales, one *smaller* than the usual effective hard-sphere radius, the appearance of such structure in these calculations is only partially consistent with our results. However, there is one important difference; these calculations base their effects on long-range ( $\lambda=2.1$ )<sup>38</sup> features while our structural anomalies have their origin in the short-range part of the effective pair potentials. Since  $\lambda=2.1$  is rather large, we would also expect anomalous structure in the small- $q$  region at low and intermediate densities. Furthermore analytic results<sup>40</sup> indicate that at high densities the effects of the repulsive step in  $\Phi(r)$  on the structure of the system should begin to disappear.



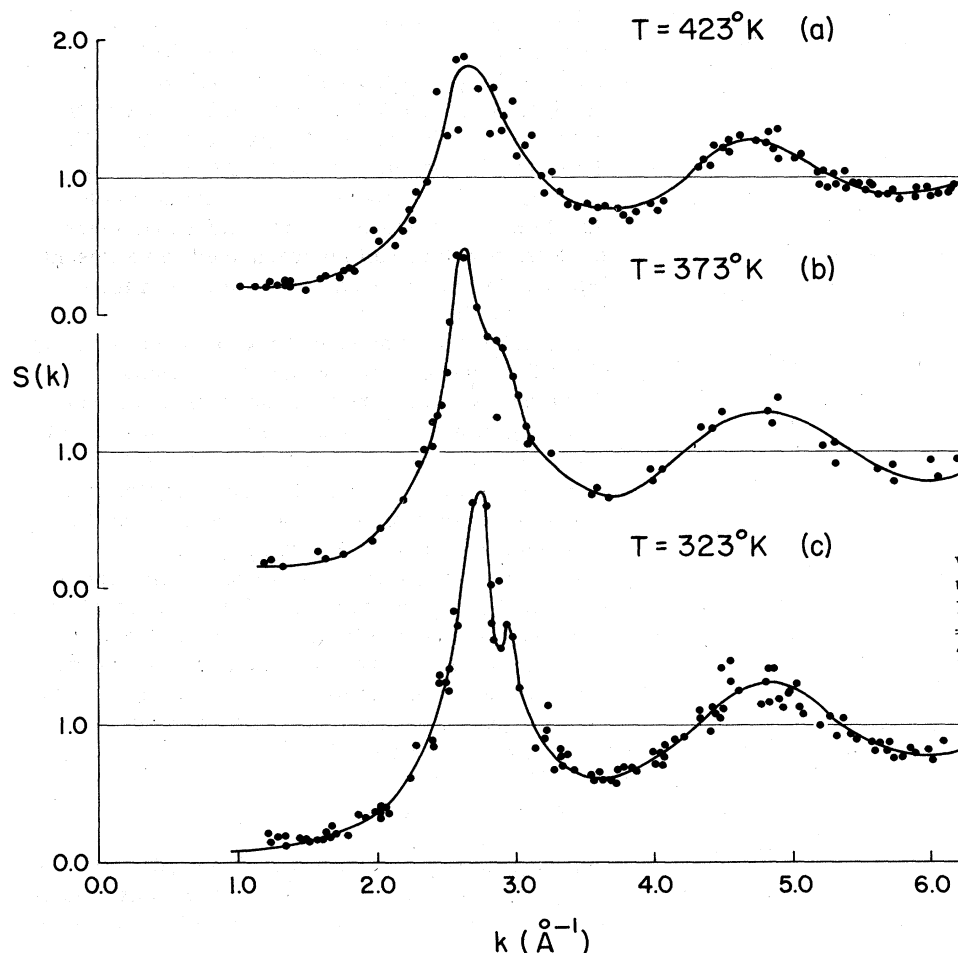


FIG. 18.  $S(k)$  calculated with the potential of Fig. 9c using systems ranging from 100–250 particles: (a)  $T = 423^\circ\text{K}$ , (b)  $T = 373^\circ\text{K}$ , (c)  $T = 323^\circ\text{K}$ .

## V. DISCUSSION

We have shown by direct Monte Carlo simulation that anomalies in  $S(k)$  very similar to those observed experimentally can occur when a model pair potential is used that displays a secondary minimum at a separation smaller than that characteristic of the primary minimum. We have also shown that in polyvalent metals whose ions are substantially polarizable an ion-ion interaction that properly includes screened fluctuating dipole interactions can develop such a secondary minimum. In the case of Ga, the screened Van der Waals interaction is a noticeable part of the entire interaction and is rather readily identified with the structural anomaly. It is also interesting to note that Ga, along with other metals in the group displaying structural anomalies, has an unusual ability to supercool. This tendency may follow quite naturally from the presence of the minor potential barrier separating a closer, but higher energy, nearest-neighbor position, from a more

distant lower-energy position. The possibility of trapping particles in an energetically metastable position may allow a transitory fraction of them to be at a locally higher density. It is worth noting that in the solid phase, Ga has but a single nearest neighbor and this is found<sup>41</sup> at a relative separation of 2.44 Å. Whether this can also be traced to the nonmonotonic feature in the potential will ultimately require an accurate calculation of the structural energies for the crystal. But it is clear that if the equilibrium properties of the solid are sensitive to such features, it is very likely that the dynamics (e.g., the phonon spectrum) will also be.

It is certainly of relevance to enquire about other possible mechanisms that might produce nonmonotonic features in a pair potential. Since the response properties of the interacting electron gas depend only on its density, any mechanism that might result from the theory of dense electron systems seems unlikely. Note, in particular that aluminum and gallium resemble each

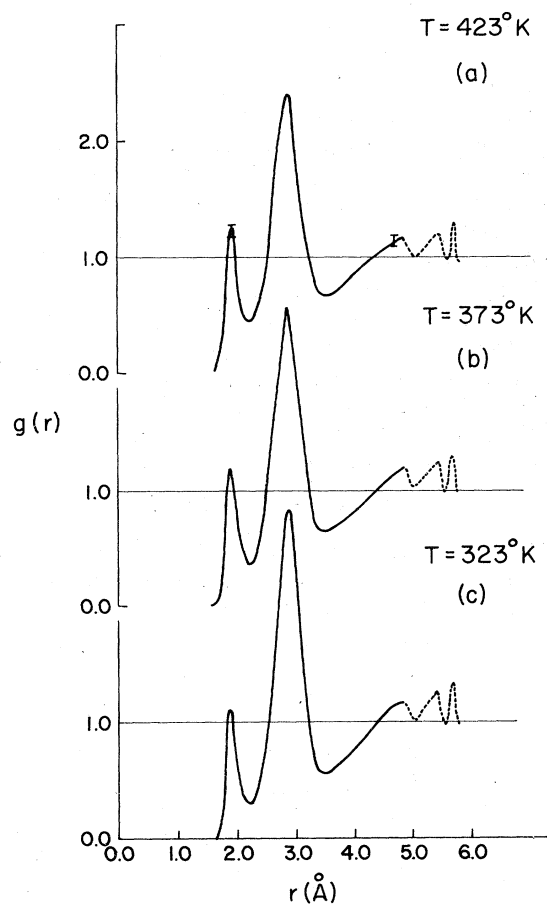


FIG. 19.  $g(r)$  calculated with the potential of Fig. 9(c): (a)  $T = 423^\circ\text{K}$ , (b)  $T = 373^\circ\text{K}$ , (c)  $T = 323^\circ\text{K}$ . Vertical bars denote typical estimated errors.

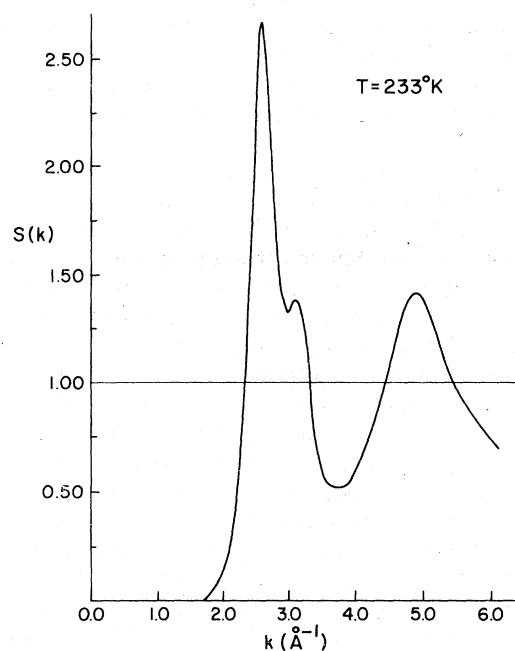


FIG. 20. Experimental measurement of  $S(k)$  for liquid Ga at  $T = 233^\circ\text{K}$  (from Ref. 8).

other very much in this respect (they have about the same electron density): yet there appears to be no anomalous structure in the observed<sup>42</sup>  $S(k)$  of liquid Al. (We note in passing that the polarizability of  $\text{Al}^{3+}$  is very small, see Table II). We may also cite evidence from alloy data. In liquid alloys such as Sn mixed with Ag where both constituents are immersed in a common electron gas, the experimental data<sup>43</sup> shows a strong subsidiary

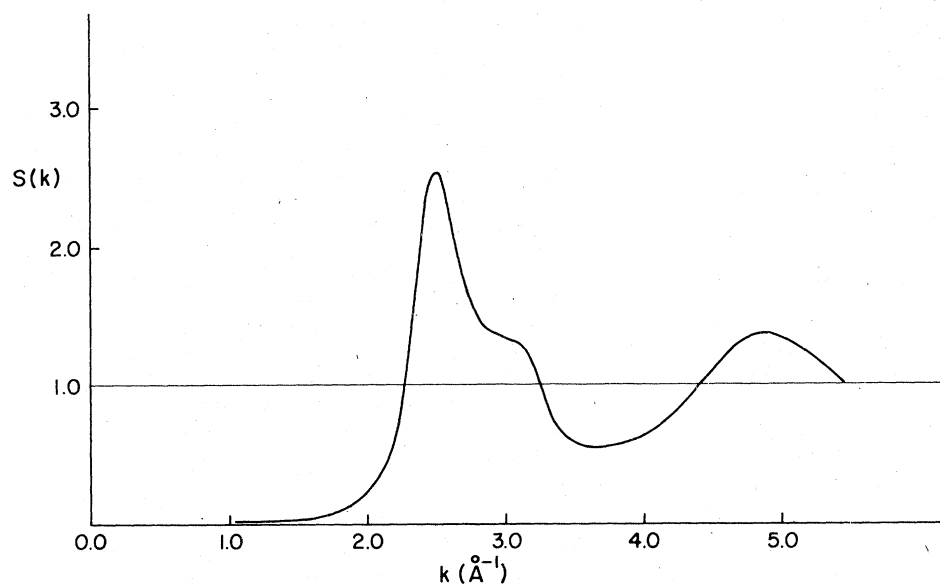


FIG. 21. Experimental measurement of  $S(k)$  for liquid Ga at  $T = 296^\circ\text{K}$  (from Ref. 8).

maximum on the principal peak of  $S_{S_{nsn}}(k)$ , asymmetry in  $S_{S_{nAg}}(k)$ , but no anomalous structure in  $S_{AgAg}(k)$ . This argues against the electron gas itself as an indirect source of the structural anomalies.

There is however, the question of three- and higher-body forces originating with nonlinear response in the electron gas. Their role in determining the equilibrium structure of liquid metals has not been fully resolved. On the other hand, if they do play a role and this is ultimately reflected as a structural feature, it is then difficult to reconcile this manifestation only with metals with filled  $d$ -electron cores, and not, for example, in others (e.g., Al) which lack this feature but otherwise have rather similar pseudopotentials. This does not dispose of many-ion forces entirely, since there are also dipole-dipole-dipole (and higher) effects going beyond the terms calculated here. But these have been estimated by Rehr *et al.*<sup>5</sup> to constitute a rather minor correction to the dominant dipole-dipole term. Perhaps more

importantly the corrections are attractive and will tend to reinforce the features we have been discussing.

Finally we may remark that in systems interacting via potentials displaying nonmonotonic features, we may anticipate thermodynamic consequences<sup>45</sup> particularly in the entropy or heat capacities, and especially at higher temperatures. Table II shows, indeed, that in just those metals with prominent structural anomalies there appears to be evidence of large excess entropies at melting. This suggests that although we have confined our attention to static structure, other thermodynamic and transport properties (and even non-equilibrium effects such as glass formation) should now be considered for this type of potential.

#### ACKNOWLEDGMENTS

This work has been supported by the National Science Foundation through the facilities of the Materials Science Center at Cornell University (DMR-76-81083, MSR Report No. 4006).

<sup>1</sup>*The Properties of Liquid Metals*, edited by S. Tekeuchi (Taylor and Francis, London, 1973).

<sup>2</sup>H. N. V. Temperley, J. S. Rowlinson, and G. S. Rushbrooke, *Physics of Simple Liquids* (Wiley, New York 1968).

<sup>3</sup>W. A. Harrison, *Pseudopotentials in the Theory of Metals* (Benjamin, Reading, Mass., 1966); *Solid State Physics*, edited by H. Ehrenreich, F. Seitz, and D. Turnbull (Academic, New York, 1970), Vol. 24.

<sup>4</sup>We are primarily concerned with short-range effects and shall not modify our pair potentials by a background dielectric constant resulting from the ions regarded as a dielectric continuum.

<sup>5</sup>N. W. Ashcroft, U. S. Natl. Bur. Stand. Spec. Publ. No. 317, I, 179, (1970); J. J. Rehr, E. Zaremba, and W. Kohn, *Phys. Rev. B* **12**, 2062 (1975); J. Mahanty and R. Taylor, *ibid.* **17**, 554 (1978); E. Zaremba and W. Kohn, *ibid.* **13**, 2270 (1976); J. Mahanty and B. W. Ninham, *Dispersion Forces* (Academic, London, 1976).

<sup>6</sup>C. A. Croxton, *Liquid State Physics—A Statistical Mechanical Introduction*, (Cambridge University, London, 1974).

<sup>7</sup>N. W. Ashcroft and J. Lekner, *Phys. Rev.* **145**, 83 (1966).

<sup>8</sup>A. H. Narten, *J. Chem. Phys.* **56**, 1185 (1972); D. I. Page, D. H. Saunderson, and C. G. Windsor, *J. Phys. C* **6**, 212 (1973); D. G. Carlson, J. Feder, and Armin Segmüller, *Phys. Rev. A* **9**, 400 (1974).

<sup>9</sup>*Liquid Semiconductors*, edited by V. M. Glazort, S. N. Chizheuskaya, and N. N. Glagoleva (Plenum, New York, 1969); S. P. Isherwood and B. R. Orton, *J. Non-Cryst. Solids*, **8-10**, 691 (1972).

<sup>10</sup>Y. Waseda and K. Suzuki, *Phys. Status Solidi B* **47**, 581 (1971).

<sup>11</sup>P. Lamparter, S. Stieb, and W. Knoll, *Z. Naturforsch.*

*A* **31**, 90 (1976).

<sup>12</sup>D. M. North, J. E. Enderby, and P. A. Egelstaff, *J. Phys. C* **1**, 1075 (1968); Y. Waseda and K. Suzuki, *Phys. Status Solidi B* **49**, 339 (1972); see also D. Jovic and I. Padureanu, *J. Phys. C* **9**, 1135 (1976).

<sup>13</sup>V. G. Rivlin, R. M. Waghorne, and G. I. Williams, *Philos. Mag.* **13**, 1169 (1966); N. C. Halder and C. N. J. Wagner, *Z. Naturforsch.* **234**, 982 (1968).

<sup>14</sup>B. F. Wingfield and J. E. Enderby, *Phys. Lett.* **27A**, 704 (1968).

<sup>15</sup>D. M. North and C. N. J. Wagner, *Phys. Lett.* **30A**, 440 (1969).

<sup>16</sup>The structure factor peaks in Tl and Pb have very small asymmetry; see D. M. North, J. E. Enderby, and P. A. Egelstaff (Ref. 12); and C. N. J. Wagner, in *Liquid Metals*, edited by S. V. Beer (Marcel Dekker, New York, 1972); and also Ref. 7.

<sup>17</sup>D. I. Page, P. A. Egelstaff, J. E. Enderby, and B. R. Wingfield, *Phys. Lett.* **29A**, 296 (1969).

<sup>18</sup>J. P. Hansen and D. Schiff, *Mol. Phys.* **25**, 1281 (1973).

<sup>19</sup>N. W. Ashcroft and D. C. Langreth, *Phys. Rev.* **159**, 500 (1967). This calculation assumes that there are no significant shifts in core energies accompanying structural rearrangements. A similar approximation (the frozen-core approximation) is being made here. It has been shown by von Barth and Gelatt (unpublished) to be valid in the sense that energies associated with departures from the frozen-core approximation are small compared with rearrangement energies.

<sup>20</sup>N. W. Ashcroft, *Phys. Lett.* **23**, 48 (1966).

<sup>21</sup>L. Dagens, M. Rasolt and R. Taylor, *Phys. Rev. B* **11**, 2726 (1975).

<sup>22</sup>D. Bohm and D. Pines, *Phys. Rev.* **92**, 609 (1953); M. Gell-Mann and K. A. Brueckner, *ibid.*

**106**, 364 (1957); also J. Lindhard, K. Dan. Vidensk. Selsk. Mat.-Fys. Medd. **28**, No. 8 (1954).

- <sup>23</sup>D. C. Langreth, Phys. Rev. 181, 753 (1969).  
<sup>24</sup>J. Hubbard, Proc. Soc. A 243, 336 (1957).  
<sup>25</sup>L. Kleinman, Phys. Rev. 172, 383 (1968).  
<sup>26</sup>A. W. Overhauser, Phys. Rev. 156, 844 (1967).  
<sup>27</sup>D. J. W. Geldart and S. H. Vasko, Can. J. Phys. 44, 2137 (1966).  
<sup>28</sup>F. Toigo and T. O. Woodruff, Phys. Rev. B 2, 3958 (1970).  
<sup>29</sup>P. Vashista and K. S. Singwi, Phys. Rev. B 6, 875 (1977); M. W. C. Dharma-Wardoun, J. Phys. C 9, 1919 (1976).  
<sup>30</sup>A. Dalgarno and W. D. Davison, Adv. At. Mol. Phys. V 2, 1 (1966).  
<sup>31</sup>A. Dalgarno, Adv. Phys. 11, 281 (1962).  
<sup>32</sup>R. Benedek, Phys. Rev. B 15, 2902 (1977).  
<sup>33</sup>J. Kollar and G. Solt, J. Phys. Chem. Solids 35, 1121 (1974).  
<sup>34</sup>R. H. Fowler, J. Chem. Phys. 59, 3425 (1973).  
<sup>35</sup>A. Rahman, Phys. Rev. A 9, 1667 (1974).  
<sup>36</sup>N. A. Metropolis, A. W. Rosenbluth, M. N. Rosenbluth, A. H. Teller, and E. Teller, J. Chem. Phys. 21, 1087 (1953); W. W. Wood and F. R. Parker, *ibid.* 27, 720 (1957).  
<sup>37</sup>J. Chihara, Prog. Theor. Phys. 50, 409 (1973).  
<sup>38</sup>M. Silbert and W. H. Young, Phys. Lett. 58A, 469 (1976).  
<sup>39</sup>D. Levesque and J. J. Weis, Phys. Lett. 60A, 473 (1977).  
<sup>40</sup>J. M. Kincaid and G. Stell, Phys. Lett. 65A, 131 (1978).  
<sup>41</sup>R. W. G. Wyckoff, *Crystal Structure*, (Interscience, New York, 1963).  
<sup>42</sup>H. Ruppertsberg and H. Wehr, Phys. Lett. 40A, 31 (1972); R. R. Fessler, R. Kaplow, and B. L. Averbach, Phys. Rev. 150, 34 (1966).  
<sup>43</sup>N. C. Halder and C. N. J. Wagner, J. Chem. Phys. 47, 4385 (1967).  
<sup>44</sup>L. Pauling, Proc. R. Soc. A 114, 191 (1927).  
<sup>45</sup>T. E. Faber, *Liquid Metals*, (Cambridge University, London, 1972).